Norwegian University
of Life Sciences

Master's Thesis 2016 30 ECTS
Department of Mathematical Sciences and Technology

Buried Flexible Structures Modeling and Field Behavior

Andrea Fæste
MTech Construction and Architecture

Preface

Seven years in higher education has come to its end, and its time to grow up. With me I bring three good years at NTNU and four even better years at NMBU. I was lucky to get a summer job at Statens Vegvesen in 2012, which lead me into the right course and the right educational pathway. With this I deliver my final assignment, all good times must come to an end.

First I would like to give tanks to my supervisor Jan Vaslestad for guidance and motivation during my work. I would like to thank the guys at Statens Vegvesen for helping me with PLAXIS 2D, especially Girum Yimer Yesuf and Murad Sani Sayd. Also a big thanks to Tor Helge Johansen which together with my supervisor brought me along on field trips to perform measurements on both the Dovre structure and Furulund bru.

All gratitude to Magnhild Skattebu for teaching me the word “the” and proof-reading.

To my mother and father for encouraging and supporting me, and for picking up the phone at 5 am. To my brother for always having my back and to my little sister for being my Baluba. Last but not least, to my fiancé Torfinn Belbo for feeding me, reading me to sleep and always bringing me morning coffee.

Abstract

The future utilization of long-span buried structures requires improved theoretical understanding of the constructions. The physical dimensions are increasing and the mechanical features grow more complex. FEM modeling serves as a good tool to explore the earth pressure and the internal forces in the steel structure.

The main goal of t his thesis is to investigate the reliability of FEM modeling compared to short- and long- term measurements, with a main focus on the the pressure distribution and internal forces in the steel structure. To perform the study two existing buried structures in Norway were examined; a horizontal ellipse and an arch footed in concrete. Measurements on the horizontal ellipse included earth pressure and deformation, and measurements on the arch included earth pressure, axial force and moment. The model was contrived in PLAXIS 2D based on theoretical material properties and structure geometry.

The earth pressure on the steel structure will increase in a long-term perspective. It is therefore preferred that the modelled earth pressure coincide this accretion. The results show overall good correspondence. At the ellipse structure the modelled arching effect was higher than measured. Laboratory tests are required in order to achieve a more accurate soil model, thereby improving the results. The modelled axial stress was inverted from the measured axial stress. The measured axial force and moment were also higher than the modelled values. The measurements are based on five locations in the steel structure and it remains unclear whether or not they represent the total stress distribution. It is likely that the modelled values present a better estimation on the stress distribution. However, further investigation and additional measurements are necessary to investigate this assumption. The measurements on deformation suggested that peaking occurred during construction. Controlled peaking in buried structures is desired when the internal stress caused by deformation don't exceed the yield point. The modelled deformation estimated that the span increased. An alternative solution for obtaining a better estimate is to insert a line-load on each backfill layer in order to imitate the compression performed during backfill.

Overall the model in PLAXIS 2D produced adequate estimations of the earth pressure and internal forces. The detailed monitoring of the construction presented in the model could prove useful in future soil-steel structures. Obtaining a representative model of the selected structures will however require some additional adjustments.

Sammendrag

For å imøtekomme utfordringer knyttet til fremtidige korrugerte stålkonstruksjoner kreves økt teoretisk forståelse. Dimensjonene blir stadig større og med det blir det byggetekniske mer innviklet. FEM modellering gir et godt verktøy til utforsking av jordtrykk og kraftpåkjenning på stålstrukturen.

Målet med denne masteroppgaven er å teste relabiliteten til FEM modellering sammenlignet med målte verdier. Det er fokusert på interaksjon mellom stålrør og friksjonsmassene og kraftpåkjenningen dette medfører. To eksisterende kulverter i Norge er testet; en kulvert med horisontal ellipse og en med bueform. Målingene på ellipsen inkluderer jordtrykk og deformasjon, og på kulvert med bueform inkluderer jordtrykk, aksialkraft og moment. Modelleringen er utført i PLAXIS 2D. Modellen er basert på teoretiske verdier og geometri.

Målingene viste at jordtrykket økte over tid. Det modellert jordtrykket viste god korrelasjon opp mot de målte verdiene. I kulverten med ellipse viste modellerte verdier høyere ”Arching” effekt enn i de målte resultatene. Dette kan være grunnet de valgte parameterne i friksjonsmassene. Tester utført på friksjonsmassene kan forbedre modellen og derav forbedre resultatene. Den modellerte aksialkrafta og moment samsvarte ikke med de målte verdiene. De målte verdiene representerer spesifiserte korrugeringer i stålkonstruksjonen og det kan diskuteres om dette gir et godt bilde på total kraftdistribusjon. For å undersøke om dette er tilfelle må flere målinger utføres på et større antall korrugeringer. Den målte deformasjonen viser at det var ”peaking” i konstruksjonen under bygging. Det er ønskelig med ”peaking” så fremt ikke deformasjonen fører til flyt i stålet. Den modellerte deformasjonen samsvarte ikke med de målte verdiene. For å bedre modellen foreslås det at at det tilføres linjelast i hvert lag for å imitere tilbakefylling.

Alt i alt ga modellen i PLAXIS 2D gode estimater. Programmet er bygget opp slik at endringer under byggeprosess kan følges, dette gir god kontroll. For å forbedre modellen til de presenterte strukturene kreves enkelte forbedringer som nevnt.

Table of Contents

List of Figures

All unreferenced figures in chapter 2, 3, 4 and Appendix 2 are designed by Andrea Fæste in the student versions of Vectorworks 2016 and ArchiCAD 19, with basis in associated references. All unreferenced photographs are taken by the author in the field. All figures in chapter 5 is produced by the author in Microsoft Excel and PLAXIS 2D.

List of Tables

List of parameters

A	Area of cross section	[m^2/m]
D	Span of the structure	[m]
E_b	Young's modulus for soil	[kN/m^2]
E_s	Young's modulus for steel	[kN/m^2]
F	Calibration factor	
I_s	Moment of inertia, steel	[m^4/m]
K_w	Shape parameter	
M_C	Calculated moment with completed backfill and cover	[kNm/m]
M_M	Measured moment	[kNm/m]
N_C	Calculated axial force with completed backfill and cover	[kN/m]
N_M	Measured axial force	[kN/m]
P_0	Oil circulation pressure	[kN/m^2]
P_A	Calliper pressure	[kN/m^2]
P_B	The difference in height between cell and pressure pump	[m]
P_C	Correlation for temperature	
Q	External load from engineered soil	[kN/m]
RP	Compression grade, Standard Proctor	%
R_s	Side radius, dependent on cross section of steel pipe	[m]
R_t	Top radius, dependent on cross section of steel pipe	[m]
S_{ar}	The arching coefficient	
W	Moment of resistance	[m3/m]
a	Length of corrugation	[m]
f_1	Function associated with the equation M_C	
f_2	Function associated with the equation M_C	
f_3	Function associated with the equation M_C	
h_c	Height of cover	[m]
$h_{c,red}$	Reduced height of cover, with consideration due to peaking	[m]
h_D	Vertical distance between the crown and the line of maximum diameter	[m]
h_{rel}	Relative height of structure	[m]
u	Horizontal deflection	[m]
w	Vertical deflection	[m]
α	Shape parameter for vertical deflection	
β	Shape parameter for horizontal deflection	
ε_b	Measured strain at the base of corrugation	[kN/m^2]
ε_t	Measured strain at the top of corrugation	[kN/m^2]
γ_b	Unit weight of the backfill soil	

γ_c	Unit weight of the cover soil	[kN/m^3]
γ_m	Safety factor	
γ_n	Safety factor	
κ	Parameter describing shape of the corrugated structure	
λ	Global stiffness of the soil steel structure	
σ_b	Tension at the base of corrugation	[kN/m^2]
σ_{ep}	Earth pressure	[kN/m^2]
σ_t	Tension at the top of corrugation	[kN/m^2]
σ_c	Soil stress at the crown	[kN/m^2]

1. Introduction

1.1. General

Despite more than a hundred years of experience, corrugated steel pipes still remain an underestimated structural shape. Experience indicates that flexible culverts correctly installed require less maintenance and are more cost-effective than similar rigid structures (Peck & Peck 1948).

In general, there are two types of steel pipes: closed pipes moulded in one piece, and pipes build up by corrugated plates. The larger structures are built up by plates (Abdel-Sayed et al. 1993). Soil-steel structures in the road sector are predominantly used as crossings and passages for trains, animals, bicycles, and agriculture. In Norway, such structures are also commonly used for avalanche protection.

Long-span flexible culverts undergo changes in stress distribution and structural deformations over time. The greatest changes occur during the first six months after construction has been finalized (Vaslestad 1990). The structural dimensions of long-span flexible metal culverts are continuously increasing and the mechanical features are growing more complex. In order to accommodate these challenges, it is necessary to strengthen the theoretical understanding and awareness during the construction process.

1.2. Aims, Goals and Restrictions

The main goal of this paper is to compare measured results to theoretical results. Measurements were performed on two existing structures, a train passage in Sjoa and an agricultural crossing in Dovre. The modeling was performed in PLAXIS 2D. Selected hand calculations are included in order to provide a basis for comparison when measurements are absent. Deflection calculations are based on Machelski et al. (2009) and calculations on axial force and moment are based on Pettersson and Sundquist (2007).

The main focus of this study is on the soil-steel interaction, and the effect on the steel structure. The model in PLAXIS was developed by the use of material properties and geometry of selected structures. The goal is to test whether the software can produce consistent accurate estimates of earth pressure, deformations and forces in the steel structures compared to short- and long-term measurements.

2. Theory

2.1. Buried Structures

Buried corrugated steel structures can be used as an alternative to conventional bridges and concrete culverts. The main advantages for building soil-steel structures include a shorter construction period, as well as the structures' large load-bearing capacity. In relation to avalanche protection the flexibility of the steel has proven favourable due to its ability to absorb the transient pressure from snow slides (Vegdirektoratet 2015).

2.1.1. Long Span Flexible Metal Culverts

A visual description of how the structures are constructed is shown in Figure 2.1. The bedding is made up from loose filling which is contoured to invert the shape of the steel pipe. Curved steel plates compose the pipe, and an example from inside the structure is shown in Figure 2.2. The steel plates can either be bolted together one at a time, be set up by rigging the base, side and top shell, or by setting up the rings independently before installation. Following the pipe construction, the dike is filled with backfill on both sides at equal pace. The final step is the cover. The thickness of the cover is determined by the vertical distance from pipe crown to the surface (Abdel-Sayed et al. 1993).

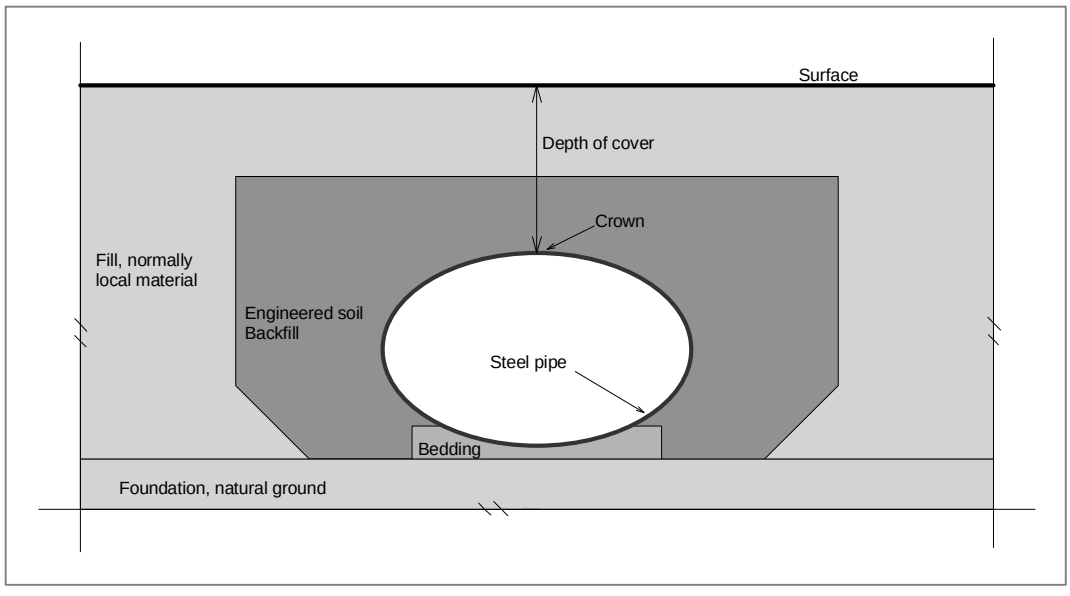

Figure 2.1. General description of a buried steel-soil structure.

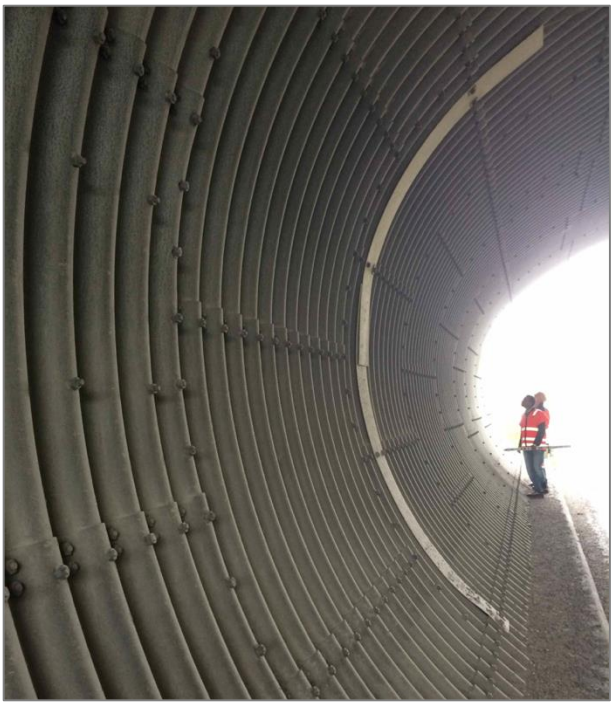

Figure 2.2. The inside of a soil-steel buried structure

The cross section of the steel structure varies according to the different areas of application. Various cross sections are illustrated in Figure 2.3. The shapes are divided into two groups; open profiles and arches. Different radii determine the structural shape. The circular pipe (2.3a) has a constant radius R. The horizontal and vertical ellipses (2.3b and 2.3c) usually have two radii, equivalent base radius R_b and top radius $R_{t,}$ and a second radius on the sides R_s. A pipe arch (2.3d) have three or four different radii, one top radius R_t, on base radius $R_{b,}$ and a corner radius R_c. Some pipe arches also have an additional side radius R_s. Arches can have a single radius R (2.3e) or three radii R_t, R_s and R_b (2.3d). A box culvert has a top radius R_t, a side radius R_s and a straight section instead of a base radius (Pettersson & Sundquist 2007).

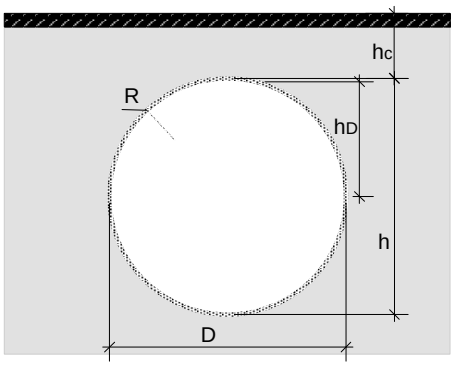

Figure 2.3a Circular pipe

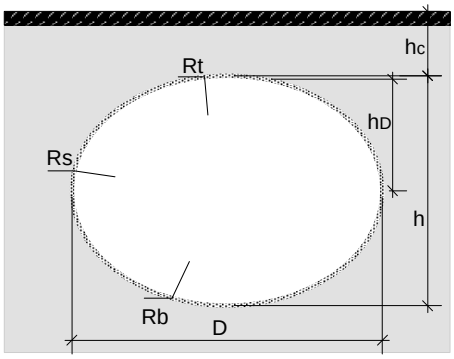

Figure 2.3b Horizontal ellipse

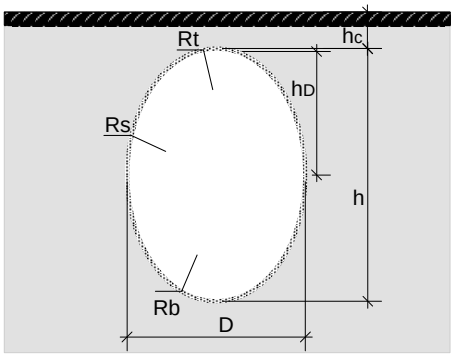

Figure 2.3c Vertical ellipse

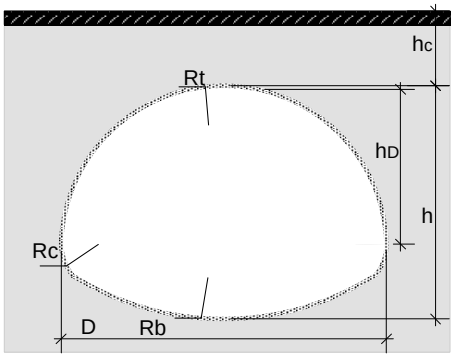

Figure 2.3d Pipe arch

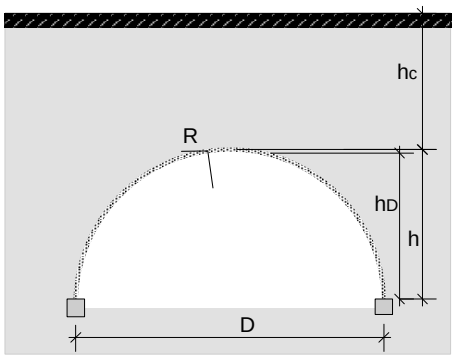

Figure 2.3e Arch, single radius

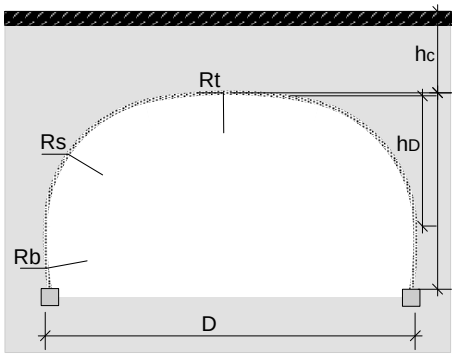

Figure 2.3f Arch, multiple radii

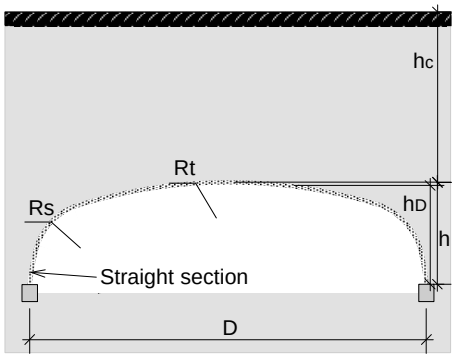

Figure 2.3g Box culvert

Figure 2.3. Cross sections of various steel structures.

The curved steel plates building the structure has a corrugation with a certain length and amplitude. The quality of the steel is S235J2 or higher. Steel plates used in Norway normally have 200x55 mm corrugation on structures smaller than 11 m in diameter, and 380x140 mm on larger ones. Corrugation is shown in

Figure 2.4. The difference between steel plates with corrugation 380x140 mm and 200x55 mm.

When corrugation is this deep, the structures can span up to 24 m. Plates interfacing the soil are refaced with corrosion protection in order to ensure an adequate lifetime (Vegdirektoratet 2015).

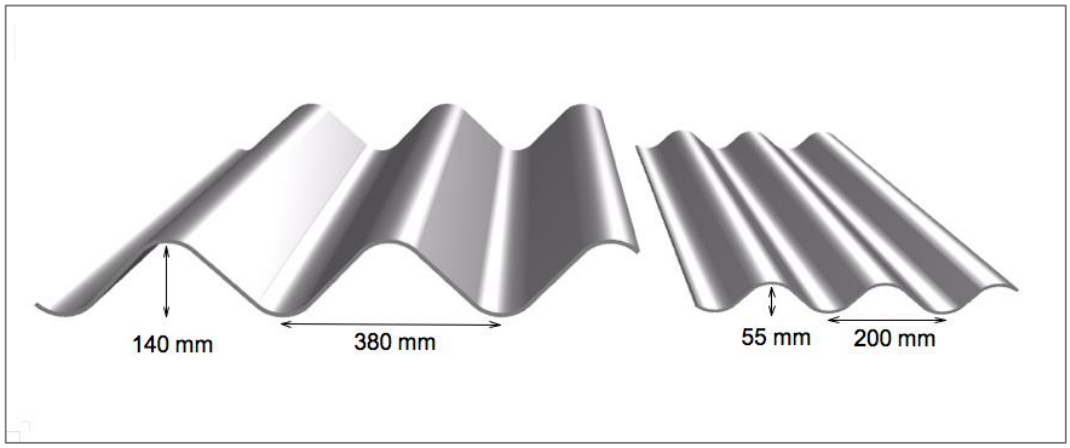

Figure 2.4. The difference between steel plates with corrugation 380x140 mm and 200x55 mm.

2.1.2. Considerations during Construction and Completion

A flexible pipe has less rigidity than the backfilling and utilizes the strength of the surrounding soil in its favour. The horizontal stress to the pipe wall is dependent on the quality and compaction of the backfilling. Correct backfilling is of utter importance when building a buried corrugated structure. If the soil is appropriately compacted the pressure will be close to uniform and hence yield small to non-existent deformations (Peck & Peck 1948; Vegdirektoratet 2015).

Positive vertical deflection, also known as peaking, is favoured during backfilling. Peaking occurs when the soil apply pressure to the steel structure and apply pressure to the side-walls. As a result, the top of the structure peak upwards as shown in Figure 2.5. Peaking is

favourable because it counteracts the posterior overburden pressure from cover and live loads. This results in a reduced bending moment and lower effective stress (Machelski et al. 2009).

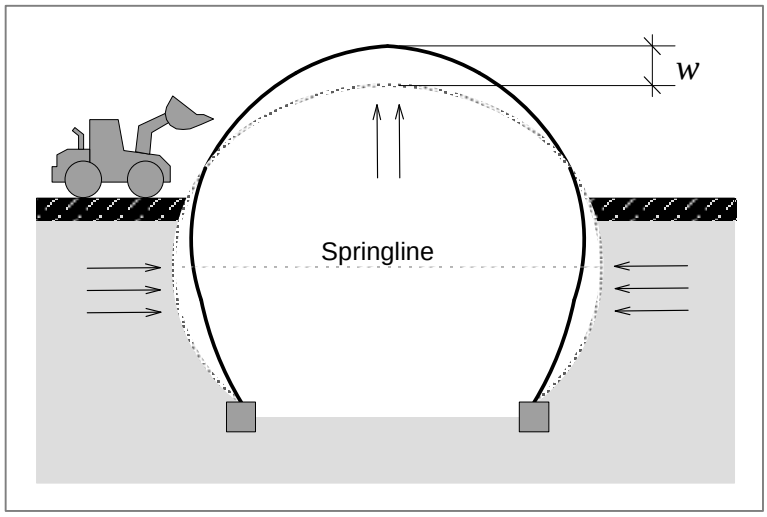

Figure 2.5. Vertical deflection w *in the steel structure caused by soil compression.*

In a long-term perspective, the earth pressure is largest around the springline. The measured values around the springline can even exceed the actual vertical overburden pressure. Former studies have shown that the horizontal earth pressure can increase up to 1.3 times of the overburden pressure, causing large stress concentrations (Vaslestad 1989).

The arching effect occurs when the soil transfers normal pressure by compression. It is thereby dependent on the soil geometry of the structure and the backfill material. The soil behaviour is difficult to predict due to diverse frictional behaviour and various boundary conditions. Positive arching results in less pressure at the crown and more on the side plates. On the contrary, negative arching results in less pressure on the sides and an accumulation of pressure at the crown (Abdel-Sayed et al. 1993; Chevalier et al. 2007; Lefebvre et al. 1976).

Arching influence different load effects uniquely and can therefore be hard to calculate. For example, the vertical earth pressure on the spring line can differ from the vertical soil pressure at the crown. The arching effect should therefore be viewed as qualitative and measured under various circumstances (Abdel-Sayed et al. 1993).

Measurements performed by Vaslestad, Kunecki and Johansen (2007) on the Dovre structure shows that the arching factor remain stable over time.

2.1.3. Recent Developments

In 2012 Atlantic Industries Limited (AIL) introduced Ultra-Cor structural plates with a 500x237 mm corrugation and plate thickness up to 12.7 mm. The new profile was developed to support heavy loads and implement broader spans then commonly used today. Deeper corrugation creates stiffer structures that can tolerate larger bending moments that counteract peaking. The new structures cause challenges concerning joints and seam strength. Thicker metal plates usually cause larger gaps, which make the structures less watertight. AIL suggest that four-sided flange connections can resolve the problem and further research is currently under progress. The flange connections also make it easier to build the pipe from the inside of the structure. This is considered safer for the constructers, as well as shortening the construction period (Williams et al. 2012).

2.2. Construction of a Corrugated Steel Culvert

Understanding the step-by-step construction of a buried structure is important in order to recognize the challenges occurring during FEM analysis.

2.2.1. Steel Structure and Fundament

Structures with a closed form need a loose soil foundation. In situations when a base plate has a radius of 4 meters or more the foundation is formed to invert the overlying structure. The template used to prepare the foundation is a pre-formed rigid shape that compresses the soil into acquired firmness. An example of a template is shown in Figure 2.6. The minimum radius of the template is 3 meters, or half of the base radius. The upper 300 mm of the foundation consist of uncompressed sand or fine gravel. The loose foundation will then mould into the corrugation thereby ensuring a stable load distribution (Vegdirektoratet 2015).

Figure 2.6. Template used to form the bedding into a desired curved form (Vaslestad 1985).

The composition of the steel structure can be performed using several methods. The most common method is to build the base, side, and top plates separately before installation. The manufacturer generally provides the specifications for the installation. A template is used to achieve the required radius (Vegdirektoratet 2015). The completed parts are lifted into place using a crane before they are joined together. Figure 2.7 shows how the base plates are placed in the inverted loose sand. After the base plate is situated the rest of the structure follows, the side plates first (as shown in Figure 2.8) and finally the top plates.

Figure 2.7. The base structure lifted with crane into the pre-formed soil (Vaslestad 1985).

Figure 2.8. The side plates bolted together with the base plates 'in situ' (Vaslestad 1985).

Arches are stabilized by the use of concrete footing. The footing has a spline adapted to the steel plates as shown in Figure 2.9. It is important to be aware of the radius of the plate segments at all time. If the radius is altered during construction the top plates will have to be forced into position. The force applied will add undesired stress in the steel structure (Vegdirektoratet 2015).

Figure 2.9. Installation of steel plates in concrete footing (Vaslestad 1997).

2.2.2. Backfill and Cover

After the steel structure is situated, the surroundings are filled with soil. The backfill is applied in layers at equal pace on both sides, and the layering should not exceed 300 mm. If the backfill is not coordinated, the distortion can cause undesired deformations in the steel structure. Each layer is compacted with selected devices to achieve the desired compaction grade. The monitoring of the compaction grade is performed with a Proctor test, and the results are compared with laboratory test on standard Proctor (Abdel-Sayed et al. 1993).

An important part of the compaction phase is the layering of soil facing the steel structure. The soil should have a lower compaction grade than the rest of the backfill and be evenly distributed in the corrugation. Achieving this delicate operation requires the use of a plate compacter as well as manual labour. A plate compacter and manual labour is shown in Figure 2.10. On the remaining backfill, larger machines like bulldozers and vibrating rollers are used for compaction, as shown in Figure 2.11 (Abdel-Sayed et al. 1993; Vegdirektoratet 2015).

Figure 2.10. Compaction of backfill with manual labour and a plate compacter (Vaslestad 1985).

Figure 2.11. Compaction of backfill with a vibration roller (Vaslestad 1985).

As the backfill rise, the steel structure is buried. Figure 2.12 shows the soil covering the crown of the steel structure. The height of the cover is dependent on the span and height of the steel structure. In some situations, it is desired to have lower minimum cover than the requirements. The solution is to insert a reliving slab to allocate the pressure from the structure crown to the side-walls (Vegdirektoratet 2015).

Figure 2.12. The final step of construction (Vaslestad 1985).

2.3. Finite Element Method

FEM modeling of buried structures is difficult due to the complexity of soils during backfill. Most of the deformation occur during backfill, and when completed the structure can tolerate large loads (Beben 2009).

2.3.1. Fundamental Theories

Soil-steel structures are usually described by three criteria: Deflection, Thrust and Buckling. The deflection criteria assume that the vertical load is uniform and distributed equally over the structure with corresponding reaction forces at the foundation. The horizontal forces are parabolically spread from 100° to the top with a maximum unit pressure resulting from the modulus of passive resistance. The Thrust criterion is based on the Ring Compression Theory. The Ring Compression Theory developed by White and Layer in 1960 states that the thrust on the structure wall is constant and reflects the overburden pressure. The Buckling criteria focus on deflection in the steel structure. Buckling is usually found at the crown of the construction but can also appear at other places depending on where the unfavourable stress concentrations occur (Beben 2009; Selig et al. 1980; Vaslestad 1990). The given criteria's focus on experience instead of an analytical model, and are therefore regarded as rather conservative (Beben 2009).

2.3.2. Challenges with FEM Modeling

When parameters are wisely selected, studies show that theoretical results have a satisfactory accuracy considering the behaviour of corrugated buried structures (Kunecki & Kubica 2004; Szajna 2007; Taleb & Moore 1999). The structure deflection and empirical measurements overall show good correspondence to the modelled and calculated results. The stress component in the contact section between soil and steel seems to be the main challenge when using FEM analyses on buried structures. The contact section is unilateral and change during backfill. The quality of the backfill depends on three factors; the soil compaction, the soil-steel interface, and the soil layering; thereby making it vulnerable to inaccuracies. Numerical estimates of axial stress occur to be higher than the actual stresses in the structure. Kunecki and Kubica (2004) suggest that springs should be applied with a specific stiffness or GAP contact elements between the soil and steel when performing analysis to resolve the problem.

GAP contact elements are two-node elements inserted between contact surfaces. These elements are divided into two groups, constant direction GAP elements and constant distance

GAP elements (Shimoseki et al. 2003). The constant GAP elements take friction into consideration and can be used for buried structures.

2.4. Method of Calculation

2.4.1. SCI-Method

Several publications on soil-steel analysis are based on the SCI-method (Soil-Culvert Interaction), first introduced by Duncan in 1977. The method is founded on the Ring Compression Theory and can be used on corrugated steel pipes and arches. The SCI- method is a finite element analysis for modeling the culvert structure and the surrounding backfill (Duncan 1978).

In later years, several modifications have been introduced to the SCI-method. Among others, these include calculations for soil modulus based on Andréasson´s work from 1973, as well as the reduction of the design normal force based on Vaslestad´s doctorial thesis from 1990 (Pettersson & Sundquist 2007).

2.4.2. Machelski, Michalski & Janusz

The global stiffness λ of all soil-steel structure can be described trough the elastic modulus, moment of inertia and metric values. (Machelski et al. 2009; Pettersson & Sundquist 2007).

$$\lambda = \frac{E_b}{E_s}\frac{a}{I_s}D^3 \tag{2.1}$$

Equation 2.1 does not restraint due to shape, radius or height of the backfilling. As a measure of precaution Machelski, Michalski and Janusz therefore proposed new equations based on the SCI method, describing both the vertical and the horizontal deflection.

The parameter κ describes the ratio between the cover height and span of the structure. From global stiffness λ and κ the shape parameter K_w is found in Figure 2.13. K_w is then used to find the metrical deflection w (Machelski et al. 2009).

$$\kappa = \frac{h_{c,red}}{D} \tag{2.2}$$

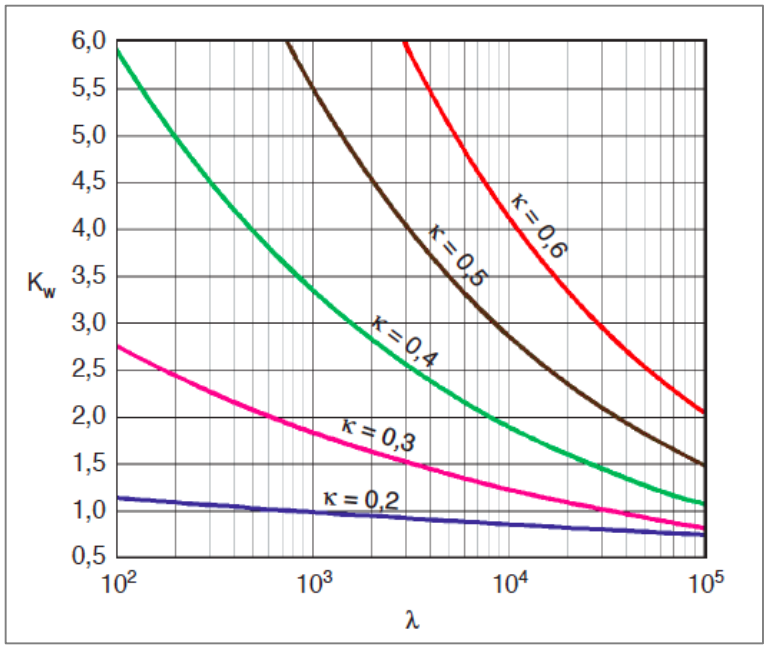

Figure 2.13. The function $K_w(\kappa, \lambda)$ (Machelski et al. 2009).

$$w = \frac{K_w}{10^5}\frac{\gamma_c a}{E_s I_s} D^5 \tag{2.3}$$

Grounded on the type of support level and geometric shape a specified shape parameters α and β is found in Figure 2.14. The vertical deflection in the crown w and maximum horizontal deflection u can be estimated from the specified shape parameters, external load Q and steel parameters (Machelski et al. 2009).

$$w = \alpha \frac{D^3}{E_s I_s} Q \tag{2.4}$$

$$u = \beta \frac{D^3}{E_s I_s} Q \tag{2.5}$$

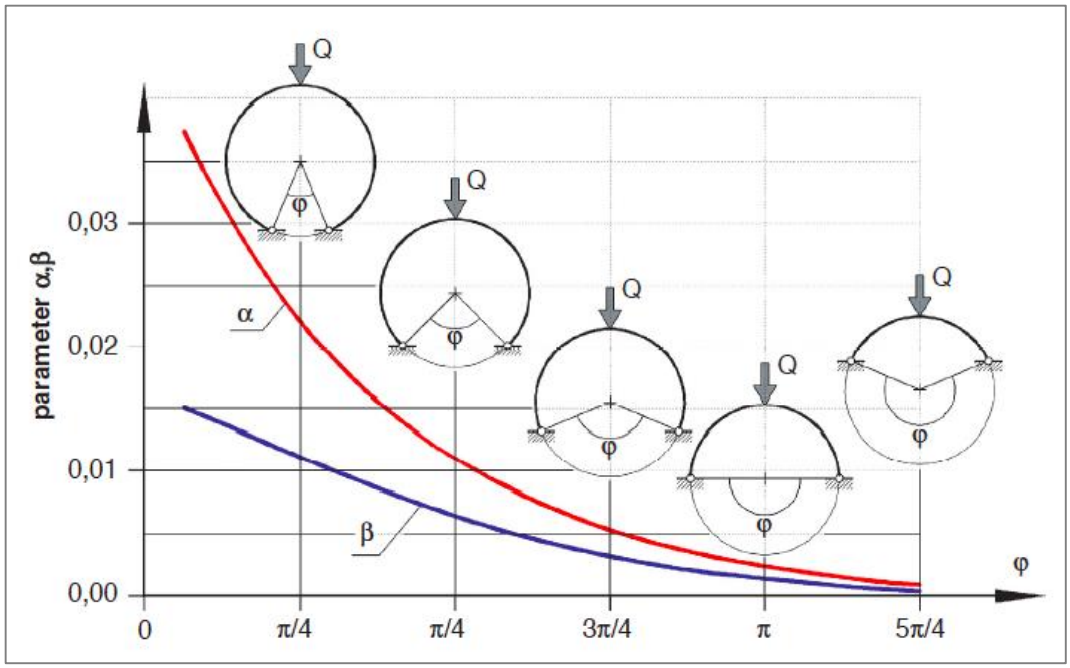

Figure 2.14 Parameters α and β as a function of geometric parameters and shape (Machelski et al. 2009).

Machelski, Michalski & Janusz performed several comparative analyses on various structures to verify their algorithm. Amongst the structures tested, the Dovre structure is included. The measured values show good correlation to the calculations, and the calculated/measured ratio for the Dovre structure was 1.01 (Machelski et al. 2009).

2.4.3. Pettersson and Sundquist

The Pettersson and Sundquist method is based on the modified SCI method. The method is quite comprehensive and in order to simplify, only axial force N_C and moment M_C due to backfill is included in this paper. The calculations are based on a structure with completed backfill and cover. The moment calculated in Eq. 2.7 is valid for conditions where $R_t \geq R_s$ (Pettersson & Sundquist 2007).

$$N_C = 0.2\frac{h_D}{D}\gamma_b D^2 + S_{ar}\left(0.9\frac{h_c}{D} - 0.5\frac{h_c}{D}\frac{h_D}{D}\right)\gamma_c D^2 \tag{2.6}$$

$$M_C = \frac{2}{3}D^3\left(-\gamma_b * f_1 f_3 f_{2,b} + S_{ar}\gamma_c \frac{h_{c,red}}{D}\left(\frac{R_t}{R_s}\right)^{0.75} f_1 f_{2,c}\right) \tag{2.7}$$

The arching coefficient S_{ar} is found from the correlation between relative cover ratio and the angle of internal friction in the cover shown in Figure 2.15. The graph is based on an algorithm established by Vaslestad (1990) (Pettersson & Sundquist 2007).

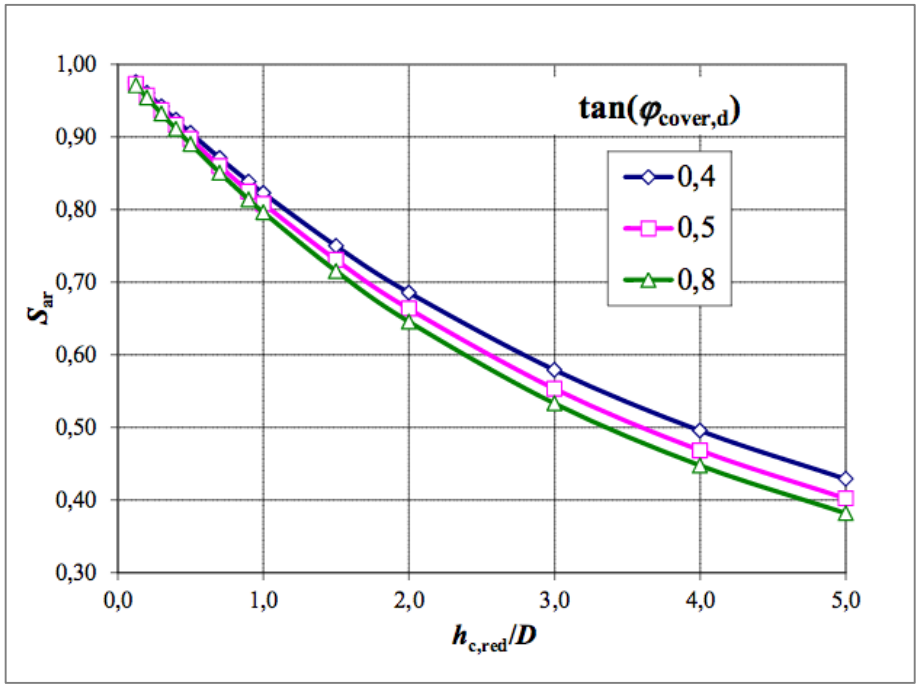

Figure 2.15. The arching coefficient S_{ar} in relation to the relative cover ratio hc,red/D and the angle of internal friction tan($\varphi_{cover,d}$) (Pettersson & Sundquist 2007).

The function f_1 is calculated by finding the ratio between the vertical distance from the crown to the line of maximum diameter and the span of the structure. The function f_2 and f_3 is dependent on the global stiffness of the soil-steel structure (Pettersson & Sundquist 2007).

$$f_1 = 0.67 + 0.87\left(\frac{h_D}{D} - 0.2\right) \quad \text{if } 0.2 < \frac{h_D}{D} \leq 0.35 \tag{2.8a}$$

$$f_1 = 0.8 + 1.33\left(\frac{h_D}{D} - 0.35\right) \quad \text{if } 0.35 < \frac{h_D}{D} \leq 0.5 \tag{2.8b}$$

$$f_1 = 2\left(\frac{h_D}{D}\right) \quad \text{if } 0.5 < \frac{h_D}{D} \leq 0.6 \tag{2.8c}$$

$$f_{2,b} = 0.0046 - 0.001 \times^{10} log\,\lambda \quad \text{if } \lambda \leq 5000$$

(2.9a)

$$f_{2,b} = 0.0009 \quad \text{if } \lambda > 5000 \tag{2.9b}$$

$$f_{2,c} = 0.018 - 0.004 \times^{10} log\,\lambda \quad \text{if } \lambda \leq 5000$$

(2.10a)

$$f_{2,c} = 0.0032 \qquad \text{if } \lambda > 5000 \tag{2.10b}$$

$$f_3 = 6.67\frac{h_D}{D} - 1.33 \tag{2.11}$$

The global stiffness λ can be calculated in different ways. The equation presented in Pettersson and Sundquist (Eq. 2.12) has a small variation from the one provided in Machelski et. al (2009) (Eq. 2.1). The safety factor γ_m is usually set to 1.3 (Pettersson & Sundquist 2007)

$$\lambda = \frac{E_b D^3}{E_s I_s}\frac{1}{\gamma_m} \tag{2.12}$$

3. Structures

3.1. Dovre

The buried structure situated in Dovre leads highway E6 under an agriculture crossing. Coordinates at 61°59´14.9”N 9°14´36.5”E. The surroundings and structure is presented in Figure 3.1.

Figure 3.1. Presentation of the Dovre structure.

3.1.1. Description

The structure consists of a horizontal ellipse with a span of 10.78 m, height of 7.13 m and a maximum cover of 4.2 m. The cross section, including a description of the soil, is illustrated in Figure 3.2. The upper part of the pipe is strengthened with concrete beams that are 1,3 m tall. The length of the structure is 24.8 m measured at the crown. The steel plates have 200x55 mm corrugation, and 7 mm thickness (Vaslestad 1987).

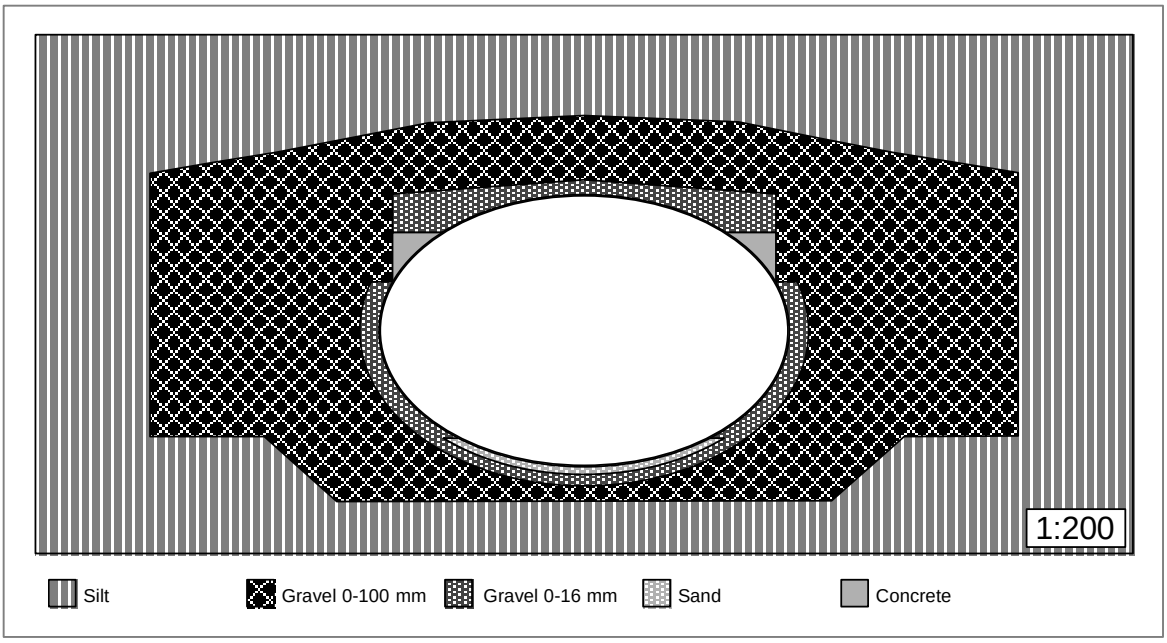

Figure 3.2. Cross section of the Dovre structure including description of the soil geometry 1:200.

3.1.2. Instrumentation

Hydraulic earth pressure cells of the type Glötzl were installed to measure earth pressure in the structure. The placement of the cells in the cross section is shown in Figure 3.3. Cell 1 lies between the bedding and the pipe, cell 2, 3, 5 and 6 are installed directly on the pipe wall, cell 4 is installed on the concrete beam, and cell 7 and 8 are placed 0.3 m and 1.5 m above the crown (Vaslestad 1987).

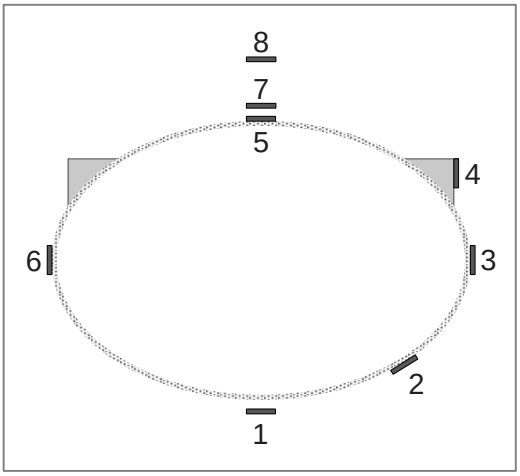

Figure 3.3. Location of earth pressure cells at the Dovre structure.

3.2. Furulund Bru

Furulund bru is a buried structure situated in Sjoa leading country road Fv257 over the railway “Dovrebanen”. Coordinates at 61°40´42.5”N 9°32´29.2”E. The surroundings and structure is presented in Figure 3.4.

Figure 3.4. Presentation of Furulund bru.

3.2.1. Description

The steel structure is an arch footed in a concrete foundation, which has a 9.5 m span and is 7.0 m tall. The cover is shallow with a minimum depth of 0.5 m, while the recommended cover for the given structure was 1.2 m. As a precautionary measure, a reliving slab was installed above the crown to distribute pressure along the sides. The concrete slab is 260 mm tall and has a 10 m span. A cross section and description of the soil geometry is illustrated in Figure 3.5. The steel plates of the structure have a 150x50 mm corrugation and 7 mm thickness (Braaten et al. 2000).

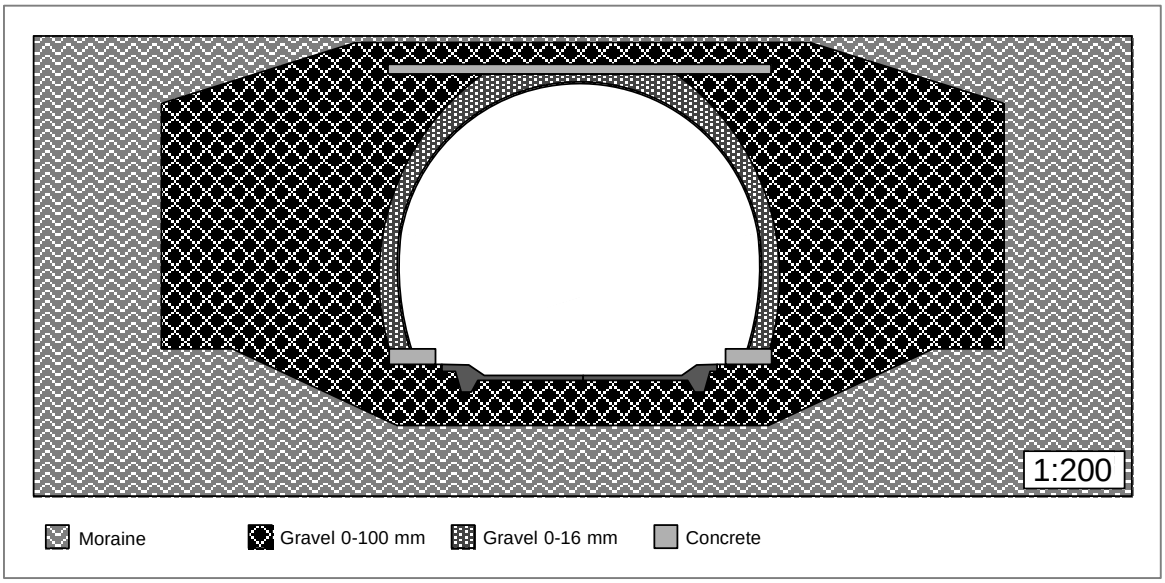

Figure 3.5 Cross section of Furulund bru including description of soils 1:200.

3.2.2. Instrumentation

Glötzl hydraulic earth pressure cells where installed in two locations. Cell 1, 2 and 3 situated 23 m from the northern opening, and cell 4 situated 27 m from the northern opening. The placement of the cells in the cross section is shown in Figure 3.6. Cell 1 and 2 is installed in the backfilling (horizontally and vertically), while cell 3 and 4 is installed directly on the pipe wall (Braaten et al. 2000).

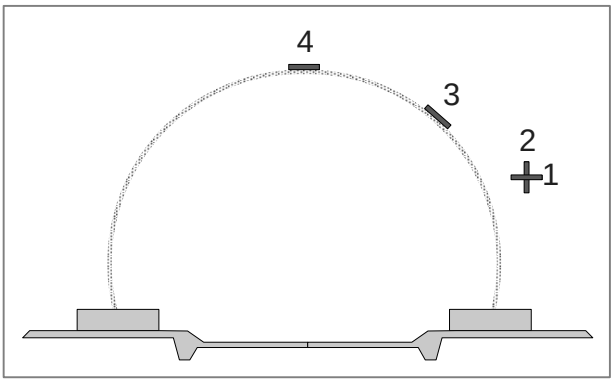

Figure 3.6. Location of the earth pressure cells at Furulund bru.

Strain gauges are installed at five locations inside circumference of the steel wall. The placement is shown in Figure 3.7. Strain gauge 3 is located in the crown, and strain gauge 2 and 4 in the side-wall. Strain gauge 1 and 5 is positioned in the footing of the steel structure.

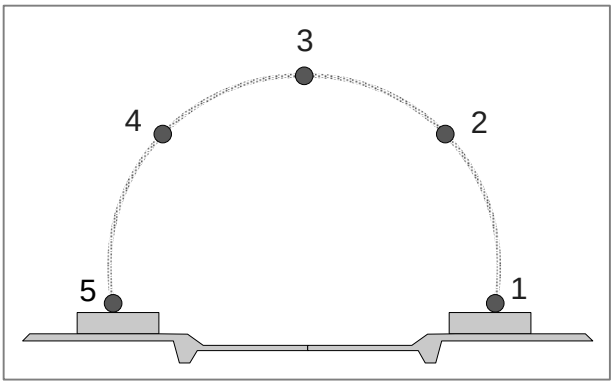

Figure 3.7 Location of the strain gauges situated at Furulund bru.

3.3. Procedure of measurement

3.3.1. Earth Pressure Cells

The measurements performed on the Dovre structure were conducted from July 1985 to June 2015. Meanwhile, the measurements on Furulund bru were frequent from 1997 to 1999, and had one supplementary measurement in 2015. In both cases the frequency of the measurements was higher during the first months of construction and settlement. Tor Helge Johansen performed the measurements and supplementary calculations on behalf of behalf of Vegdirektoratet.

Glötzl hydraulic earth pressure cells measures pressure from oil P_0 circulating trough the cell. The earth pressure depends on the internal pressure in the instrument P_A, and the difference in height between instrument, cell and temperature correlation P_C (Kunecki et al. 2006).

$$\sigma_{ep} = \frac{P_A + P_B - P_C - P_0}{F} \tag{3.1}$$

3.3.2. Strain Gauges

The strain measurements on Furulund bru were performed since the beginning of the construction in 1997 to September 1999. Tor Helge Johansen performed the measurements and alteration to tension on behalf of Vegdirektoratet.

Measurements of tension in the steel pipe are achieved using strain gauges. The strain is measured in the top and base of the corrugation. The tension at the top and base of the corrugation is decided from the measured strain ε_t and ε_b and the Young´s modulus for steel E_s (Vaslestad 1987).

$$\sigma_t = \varepsilon_t \times E_s \quad (3.2)$$

$$\sigma_b = \varepsilon_b \times E_s \quad (3.3)$$

Subsequently the axial force and moment is calculated from the tension parameters, cross section *A* and the moment of resistance *W*. Temperature must be taken into consideration when operating with strain gauges, since it may alter the results (Vaslestad 1987).

$$\mathrm{N_M} = \frac{\sigma_t + \sigma_b}{2} \times \mathrm{A} \quad (3.4)$$

$$M_M = \frac{\sigma_t - \sigma_b}{2} \times W \quad (3.5)$$

3.3.3. Deformation

The horizontal deformation is measured inside the steel pipe on selected positions. The measurements are performed with an electronic desistance instrument. To confirm that the placement of the measurement is at correct height, a gauging rod is applied to the wall. Several measurements are performed at the same site to ensure validity.

4. Method

4.1. Measurements

The measurements were obtained from Tor Helge Johansen on behalf of Vegdirektoratet.

4.1.1. Earth Pressure

The measurements on earth pressure on the Dovre structure and Furulund bru include values measured since the initiation of construction until the last measurements were conducted in 2015. The results are presented graphically. The reading of the measurements focuses on variations in the construction phase, and the long-term development. At the Dovre structure the earth pressure in cell 2, 4, 7 and 8 present no further significance to the analysis and is found in Appendix 1.

4.1.2. Axial Stress and Moment

Measurements on the tension in the Furulund bru structure include results from the construction. Axial force and moment was calculated with equation 3.4 and 3.5 and the results are presented graphically.

4.1.3. Deformation

Measurements on horizontal deformation in the Dovre structure include measured values from the beginning of construction to the last measurements in 2015. The results are presented diagrammatically. The reading of measurements focuses on maximum deformation during construction and stabilization in a long-term perspective.

4.2. PLAXIS 2D

The Dovre and Furulund bru structures were modelled in PLAXIS 2D. The software is based on the Finite Element Method using material properties, geometry and mesh to obtain results. Material properties and cross sections with format 1:100 are presented in Appendix 2.

4.2.1. Material Properties

When selecting soil parameters, the main focus is on the backfill. The Mohr Coulomb model is chosen because of its quality to capture the response of the loads on the structure caused by friction masses (Wadi 2012). The model is favourable for friction masses when in absence of

exact soil parameters. More exact soil parameters can be decided in a laboratory by doing experimental test, for instance a direct shear test or a triaxial test.

Young´s modulus of the backfill and cover is calculated with Eq. 4.1 (Vegdirektoratet 2015).

$$E_b = \frac{1.2}{\gamma_n} 1.17^{RP-0.95} \left[1.25\, ln\, h_c + \frac{h_D}{2} + 5.6\right] \quad (4.1)$$

4.2.2. Geometry

The geometry is based on coordinates from previous reports, drawings and descriptions. The 'in situ' soil is placed before then the foundation and backfill is inserted as soil polygons. The concrete beam in the Dovre structure is embedded as a soil polygon with itemized parameters. The concrete material is set as a non-porous material with linear elastic features. Geometric properties for ellipsoid and arches are not programmed in PLAXIS 2D, and must be imported from another program. Soil polygon coordinates can be plotted in Microsoft Excel and imported as a text file. At Furulund Bru the description of the structure was vague. The geometry and soil parameters were derived from Håndbok 220 (2014) as well as the obtained experience from the programming of the Dovre structure parameters.

The tunnel ellipse is made out of an ellipse with three radii. A good estimation of the given ellipse is obtained from illustrations and manual testing. The steel arch has two radii. A fixed line displacement in x- and y-direction is attached in the footing. Each segment in the steel structures is given attributes such as plate, positive and negative interface, and plate material.

After the model is completed the construction is meshed with desired accuracy. A fine mesh near the steel structure is desired to obtain adequate results of deformation.

4.2.3. Staged Construction and Calculation

The structure is divided into segments of 300 mm to imitate the soil layering in field during construction. Each layer is given a phase with associated soil parameters. The interface between the steel plates and soil is given individual parameters with non-rigid properties. The steel structure is specified as an own phase and applied after the fundament is placed.

The program calculates each phase individually based on the specified mesh. The results from the Dovre structure are presented in the final phase. At Furulund bru the structure has a minimum cover of 0.5 m, with a recommended cover of 1.2 m. The structure was tested for both the minimum and the recommended cover to see how it reacted.

The earth pressure is gathered from the Cartesian effective stress in x- and y-direction. Cell 1 and 2 at Furulund bru is assumed situated 500 mm from the steel structure in the interface between Gravel 0-16 and Gravel 0-100. Cell 3 is assumed situated at an angle of 45°.

4.3. Hand calculations

All parameters, assumptions and calculated results are presented in Appendix 3. The calculations on deformation are given in absolute values.

4.3.1. Estimated Axial Force and Moment

The axial force was calculated with Eq. 2.6 and the moment was calculated with Eq. 2.7. In order to simplify, the arching coefficient is adopted from Figure 2.15 and not from the algorithm by Vaslestad (1990).

4.3.2. Estimated Deformation

The vertical deflection in the crown is calculated with equation 2.3, while the horizontal deformation is calculated with equation 2.5. The shape parameter α was achieved by combining Eq. 2.3 and 2.5. The reading of the shape parameter β was subsequently obtained from Figure 2.14. The estimations exclude the concrete beams at the Dovre structure and the reliving slab at Furulund bru. At the structure Furulund bru the cover is assumed at 1.2 m.

5. Results

5.1. Dovre

5.1.1. Measurements

The horizontal earth pressure measured in cell 3 is presented in Figure 5.1. The estimated overburden pressure from overlying soil is 140 kN/m^2. During construction the earth pressure had a top value of 151 kN/m^2, and decreased to 112 kN/m^2 at completion. In the first two years the earth pressure increased to 206 kN/m^2, equivalent to 147% of the overburden pressure. The earth pressure is relatively stable in a long-term perspective and in the summer of 2015 the measured value was 210 kN/m^2.

The horizontal earth pressure measured in cell 6 is presented in Figure 5.2. The overburden pressure is estimated at 139 kN/m^2. After the structure was completed in 1985 the earth pressure was measured at 77 kN/m^2, with a peak value of 147 kN/m^2 during the construction. The earth pressure increased to 182 kN/m^2 in 2015, equal to 131% of the overburden pressure. Notice that the horizontal earth pressure measured in cell 3 is overall higher than the measurements in cell 6, though they were both placed in the same angle and height on the steel wall.

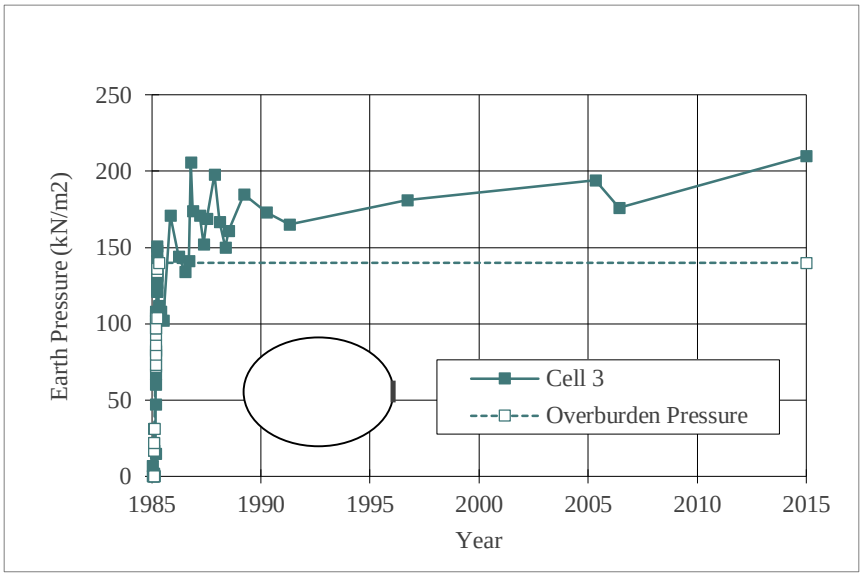

Figure 5.1. Measurements of earth pressure in cell 3 on the Dovre structure.

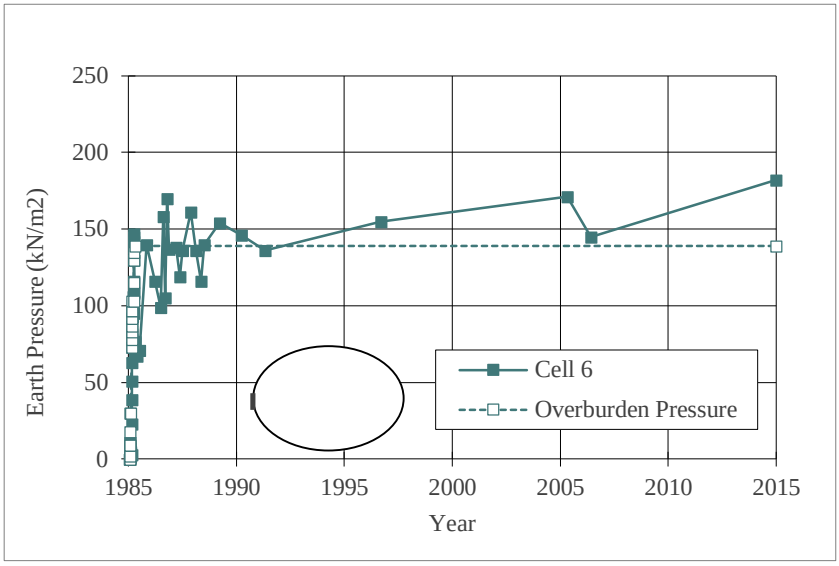

Figure 5.2. Measurements of earth pressure in cell 6 on the Dovre structure.

The vertical earth pressure measured at the crown is presented in Figure 5.3. The estimated overburden pressure is 70 kN/m^2. After construction, the measured value was 48 kN/m^2. The values measured correspond with the overburden pressure and are stable over time.

The earth pressure cell placed in the sand underneath the steel structure is presented in Figure 5.4. The estimated overburden pressure is 104 kN/m^2. The vertical earth pressure in the foundation shows little alteration over time. The measured value in 2015 was 28 kN/m^2, accordingly 27% of the overburden pressure.

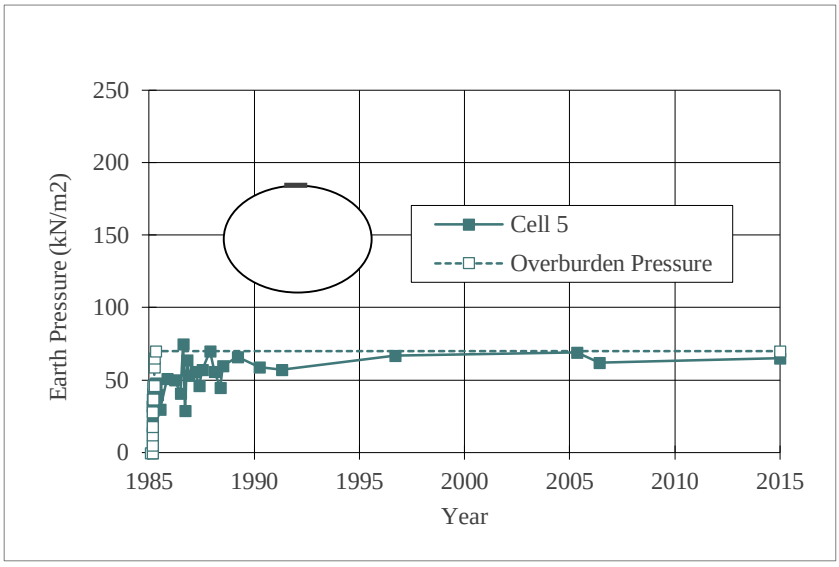

Figure 5.3. Measurements of earth pressure in cell 5 on the Dovre structure.

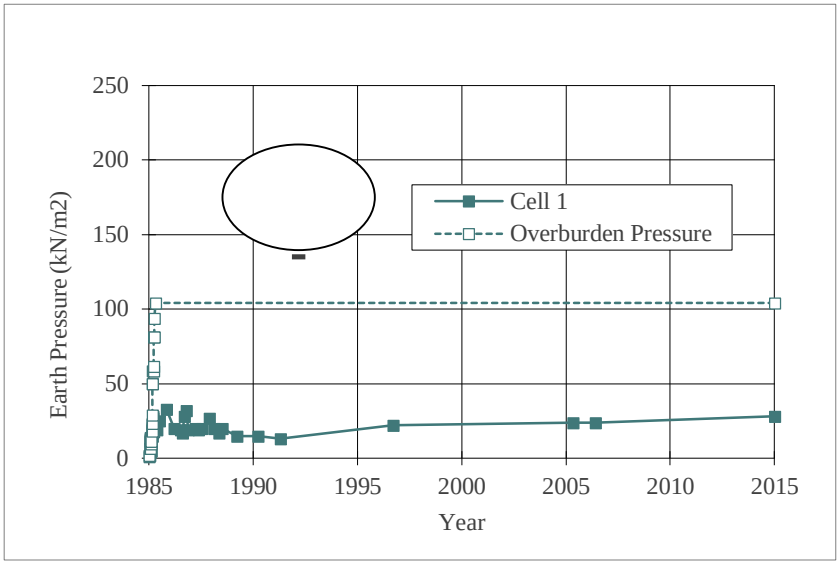

Figure 5.4. Measurements of earth pressure in cell 1 on the Dovre structure.

The measured horizontal deformation inside the pipe is presented in Figure 5.5. The negative deformations decrease the width of the span. During construction the horizontal deformation had a peak value of -35 mm. After the structure was completed the deformation stabilized on -21 mm. In 1997 the deflection decreased to -8 mm, and the same value was obtained in 2015. In the time between 1997 and 2015 the measurements varied from -8 to -16 mm. The measurements were performed in September, October, November and February, and it appears to be no correspondence between measurements done in the same month.

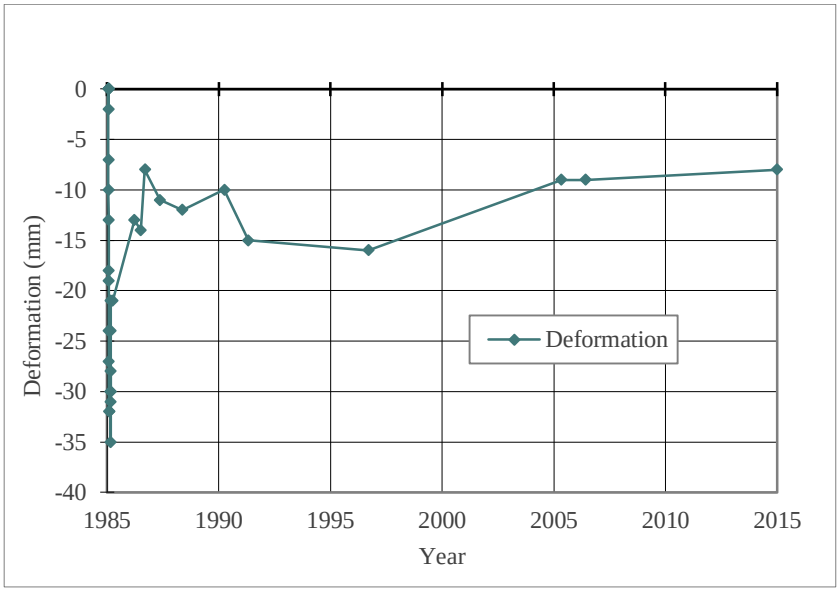

Figure 5.5. Horizontal deformation in the Dovre structure, measured inside the steel structure.

5.1.2. Modeling with PLAXIS 2D

The final geometry before calculation is presented in Figure 5.6 and Figure 5.7 shows the structure after calculation. The negatively and positively marked circles indicate the interface. The origin is placed in the centre of the structure in y-direction and parallel to the road embankment in x-direction.

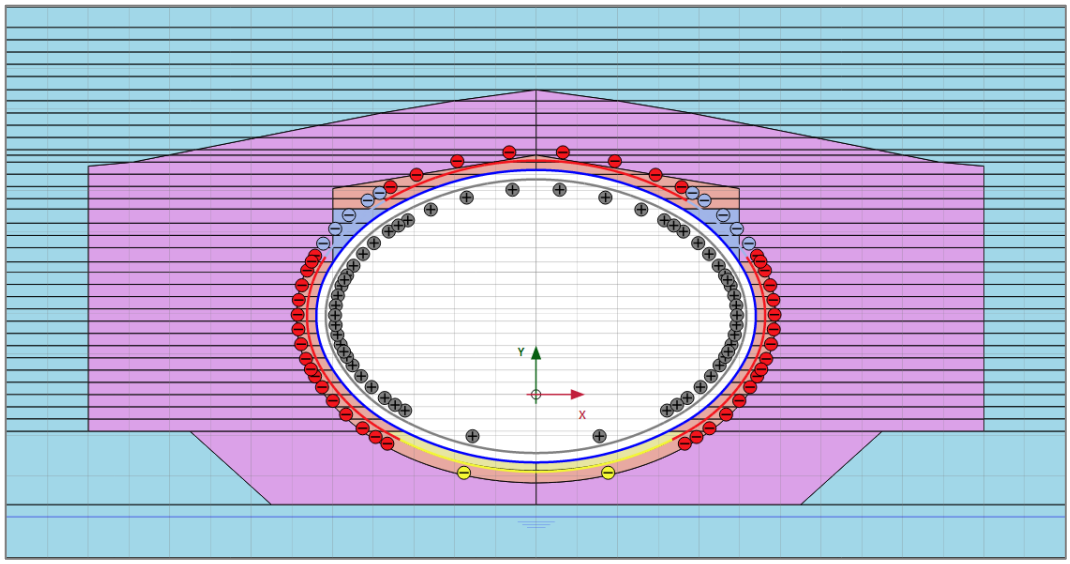

Figure 5.6. Final geometry of the Dovre structure modelled in PLAXIS 2D.

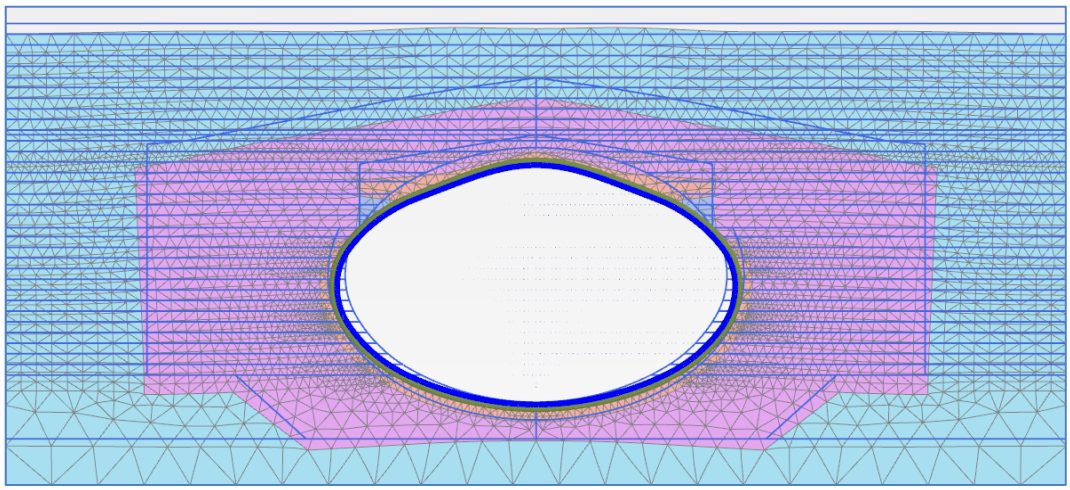

Figure 5.7. The Dovre structure after completed calculations, including deformed mesh.

The modelled earth pressure is presented in Table 1. Cell 3 and 6 show almost identical values, subsequently horizontal earth pressure of 233.5 kN/m^2 and 233.9 kN/m^2. The vertical earth pressure in the crown has a modelled value of 28.2 kN/m^2 and beneath the structure the vertical earth pressure is 40.8 kN/m^2.

Table 1 Modelled earth pressure in the Dovre structure.

	Soil	X [m]	Y [m]	σ_{ep} [kN/m^2]
Cell 3	Gravel 0-16	5.50	1.93	233.5
Cell 6	Gravel 0-16	-5.50	1.93	233.9
Cell 5	Gravel 0-16	0.00	5.61	28.2
Cell 1	Sand	0.00	-1.67	38.0
	Sand	0.00	-1.87	40.8

The modelled axial force in the steel structure is presented in Figure 5.8. The highest absolute axial force is found in the side-walls of the steel structure with a value of 554.8 kN/m. The lowest absolute axial force is found under the concrete beams with a value of 152.6 kN/m.

The modelled moment in the steel structure is presented in Figure 5.8. The maximum moment is found in the roofing with a value of 4.9 kNm/m. The minimum moment is found in the side-walls with a value of -5.7 kNm/m.

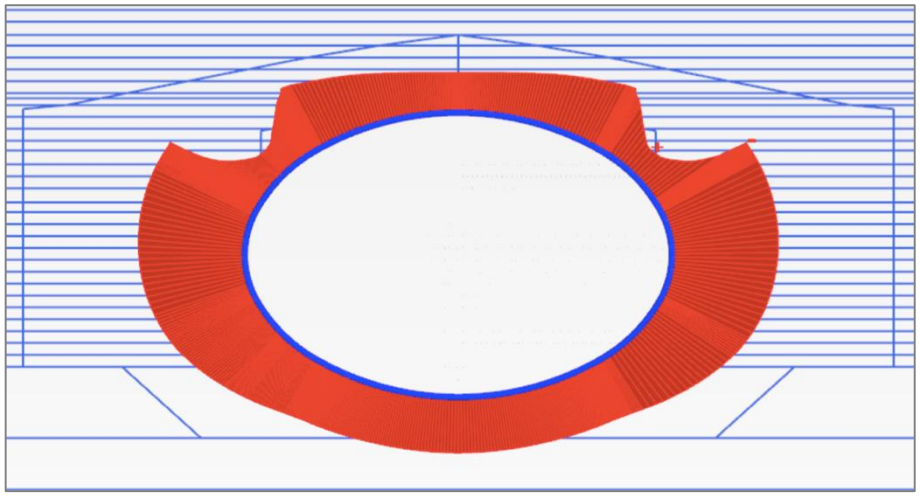

Figure 5.8. Modelled axial force in the Dovre structure

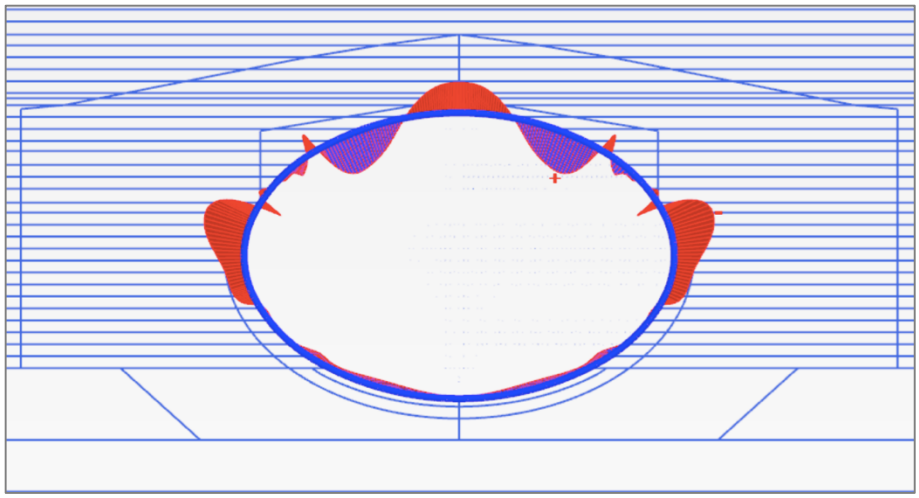

Figure 5.9. Modelled moment in the Dovre structure.

The vertical deformation in the steel structure is presented in Figure 5.10. The maximum vertical deformation is found in the crown with a value of -32.4 mm. In the crown the modelled deflection is -24.8 mm.

The horizontal deformation in the steel structure is presented in Figure 5.11. The maximum deformation is found in the side-walls with a value of 11.7 mm. The modelled deformation is positive, indicating that the span increased.

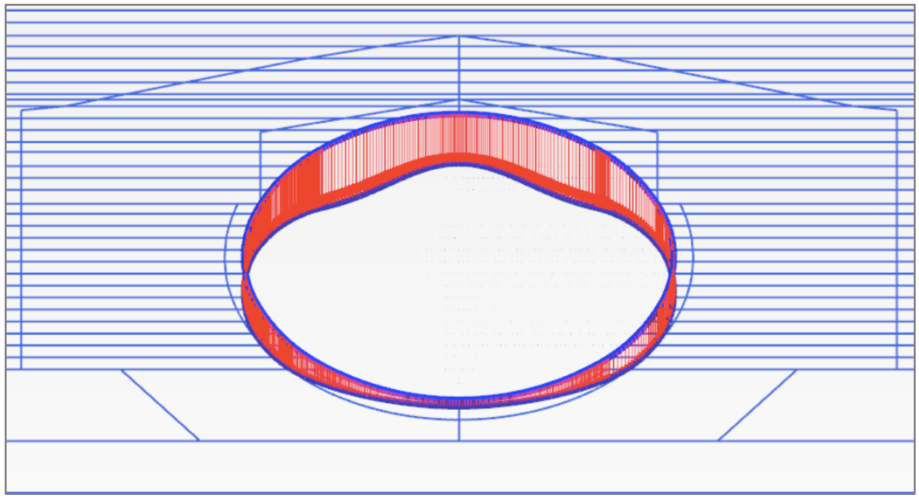

Figure 5.10. Modelled vertical deformation in the Dovre structure. Scaled up 50 times.

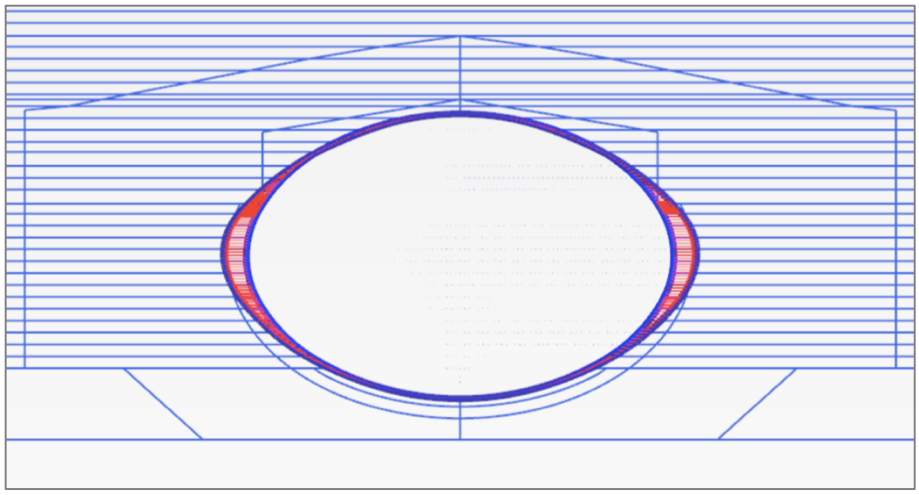

Figure 5.11. Modelled horizontal deformation in the Dovre structure. Scaled up 50 times.

5.1.3. Final Results

A systematisation of the results is presented in Table 2.

Table 2 Systematisation of result for the Dovre structure.

	Measured value after completed structure	Measured value, summer 2015	Modelled values in PLAXIS 2D	Hand calculations	
Earth pressure Cell 3	112.0	210.0	233.5	-	kN/m^2
Earth pressure Cell 6	77.0	182.0	233.9	-	kN/m^2
Earth pressure cell 5	48.0	65.0	28.2	-	kN/m^2
Earth pressure Cell 1	21.0	28.0	40.8	-	kN/m^2
Axial force	-	-	554.8	461.8	kN/m
Moment	-	-	-5.7	6.5	kNm/m
Crown, vertical deformation	-	-	-24.8	22.7	mm
Horizontal deformation	-21.0	-8.0	11.7	13.1	mm

5.2. Furulund bru

5.2.1. Measurements

The horizontal earth pressure measured in cell 2 is presented in Figure 5.12. The overburden pressure is estimated to 80.8 kN/m^2. During construction the measured earth pressure increased to 11 kN/m^2. After the structure was completed the horizontal earth pressure stabilized on 13 kN/m^2, and the same value was obtained in 2015. This value is equivalent to 16% of the overburden pressure.

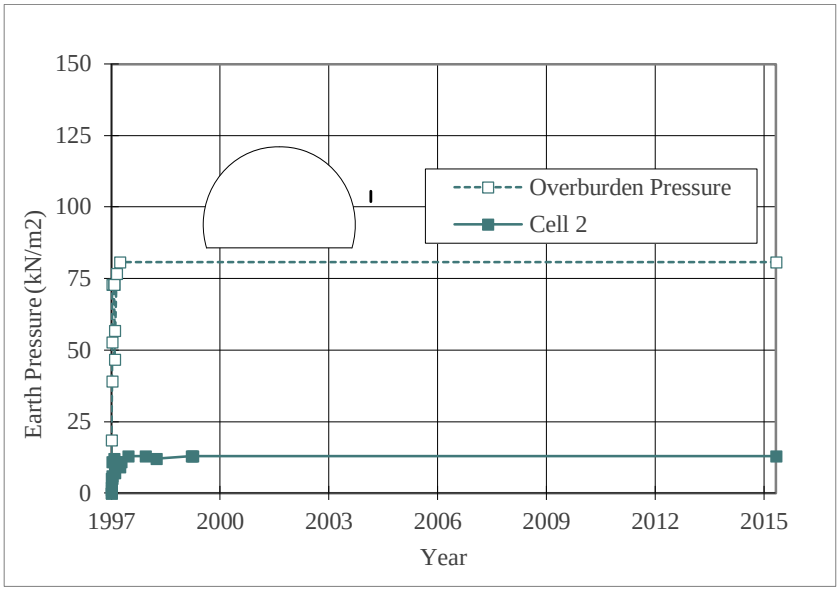

Figure 5.12. Measurements of earth pressure in cell 2 on the Furulund bru structure.

The vertical earth pressure measured in cell 1 is presented in Figure 5.13. The overburden pressure is estimated to 80.6 kN/m^2. After the structure was completed the vertical earth pressure was measured to 119 kN/m$^{2.}$ and the peak value was 127 kN/m^2 during construction. In 2015 the vertical earth pressure had increased to 136 kN/m^2, equal to 169% of the overburden pressure.

The vertical earth pressure in the crown is presented in Figure 5.14. The estimated overburden pressure is 18 kN/m^2. Following the completion of backfill and cover the vertical earth pressure was measured to 0 kN/m^2, and the peak value was 27 kN/m^2 during construction. In the years between 1998 and 2015 the measured values were stable. The measurement performed in 2015 show 9 kN/m^2, equal to 50% of the overburden pressure.

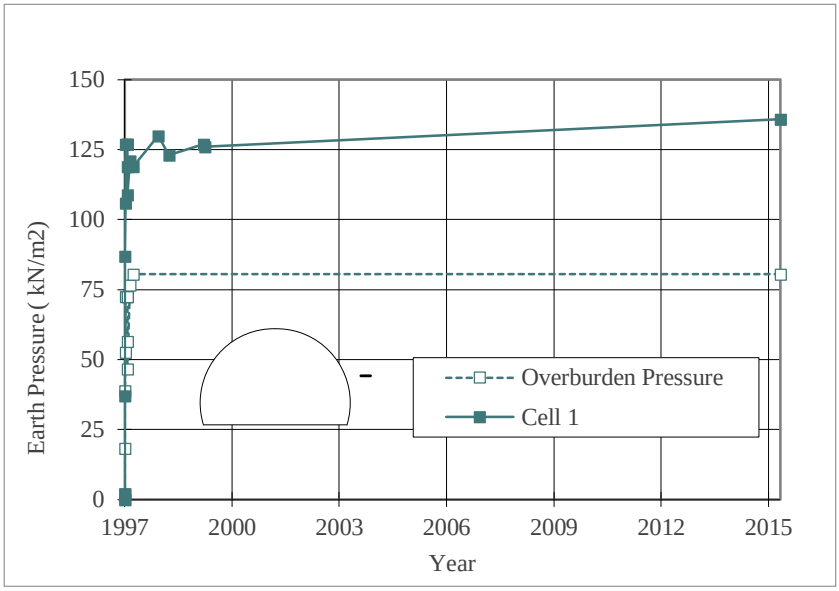

Figure 5.13. Measurements of earth pressure in cell 1 on the Furulund bru structure.

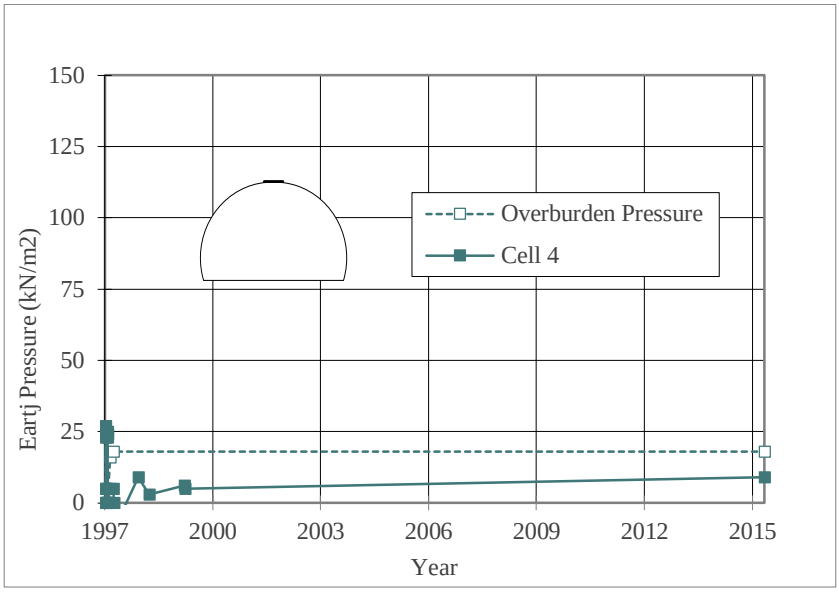

Figure 5.14 Measurements of earth pressure in cell 1 on the Furulund bru structure.

The earth pressure measured in cell 3 is presented in Figure 5.15. The overburden pressure is estimated to 45.6 kN/m^2. During construction and the latter two years the measured earth pressure stabilized on a value slightly above the overburden pressure. The 2015 measurement show a doubling of value with an earth pressure measured at 94 kN/m^2. This is equivalent to 206% of the overburden pressure. The measurement is questionable, and is excluded from further analysis.

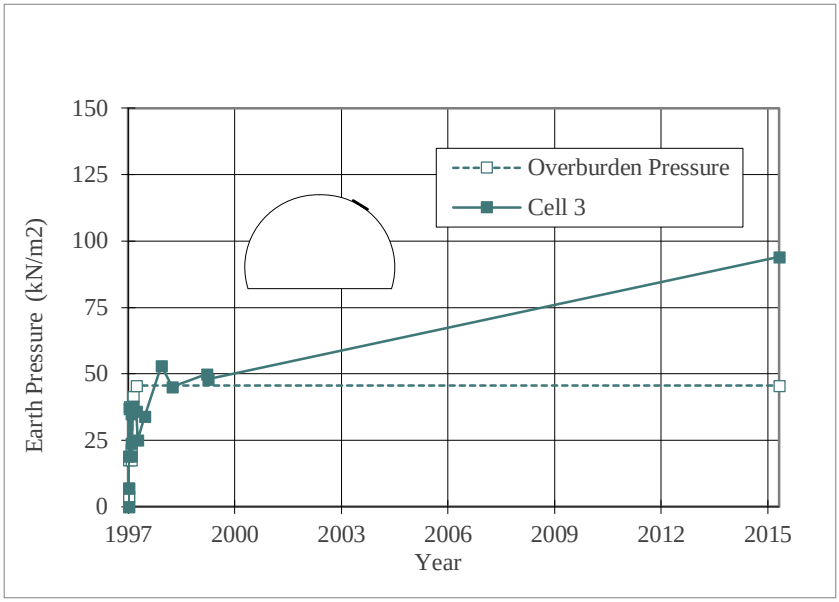

Figure 5.15. Measurements of earth pressure in cell 3 on the Furulund bru structure.

The measured axial force measured in the crown is presented in Figure 5.16. Throughout the construction period the axial force increased from 280 kN/m to 162 kN/m before settling on 333 kN/m after completion.

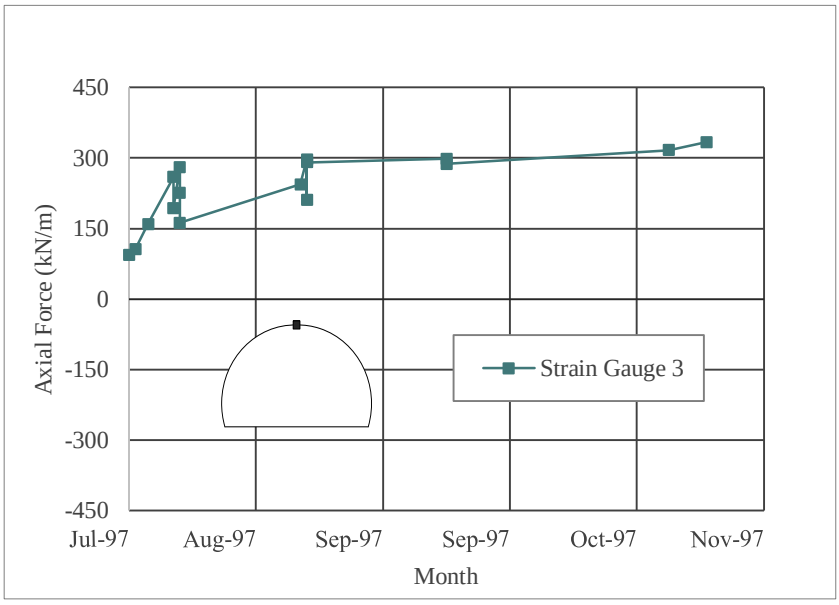

Figure 5.16 Axial force measured in strain gauge 3 in the Furulund bru structure.

The axial force on the side-wall is presented in Figure 5.17. The strain gauges are both positioned in the same height; the axial force measurements are, however, inconsistent. At completed construction the lowest measurements are found in strain gauge 4 with a value of 178.4 kN/m, corresponding to the value measured in strain gauge 2 is 36.6 kN/m. In the initiation of the construction period strain gauge 4 shows a value of 440 kN/m corresponding 38 kN/m in strain gauge 2. The large variance between the two suggests that the value 440 kN/m can be excluded from further analysis.

The axial force in the steel wall near the footing is presented in Figure 5.17. The measurements are consistent. At completed construction the measured axial force was 61 kN/m.

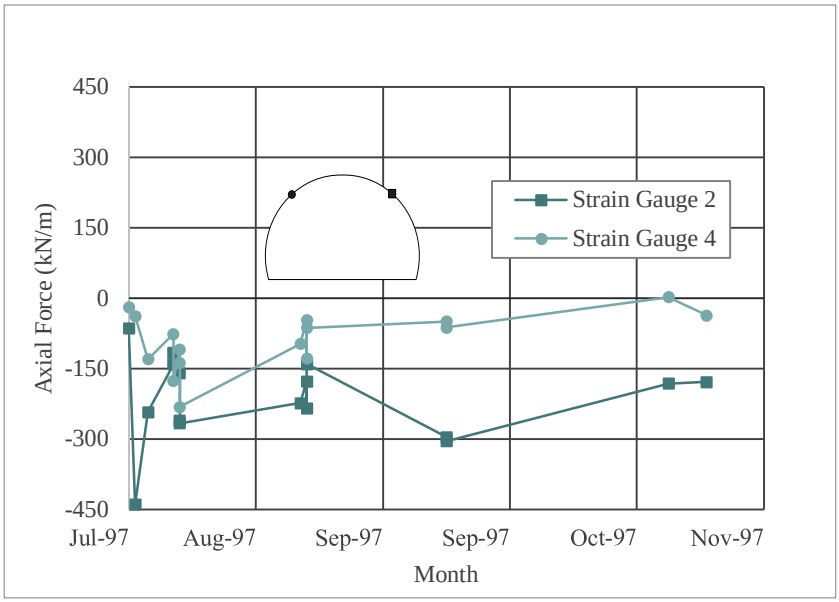

Figure 5.17. Axial force measured in strain gauge 2 and 4 in the Furulund bru structure.

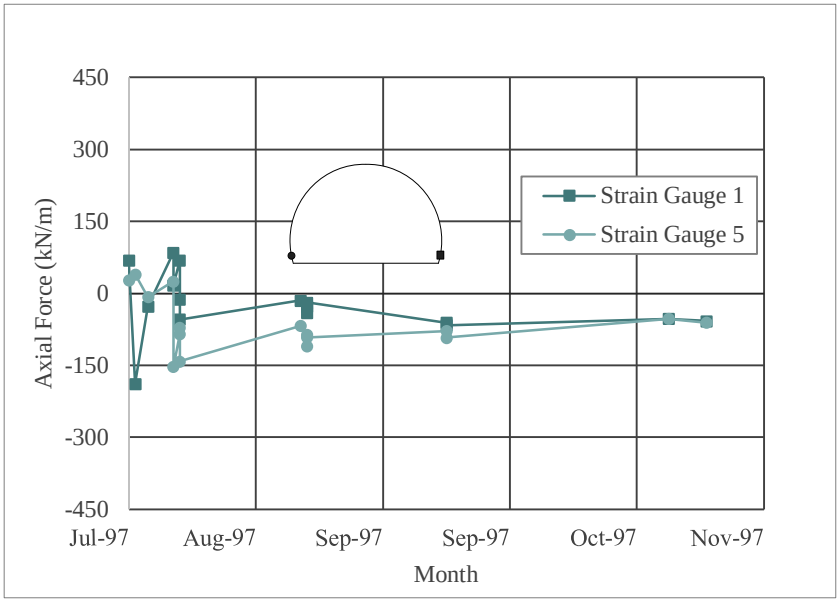

Figur 5.18 Axial force measured in strain gauge 1 and 5 in the Furulund bru structure.

The measured moment in the crown is presented in Figure 5.19. After completion the moment stagnated on a measurement of 20.1 kNm/m. During the construction the moment had a peak value of 22.5 kNm/m.

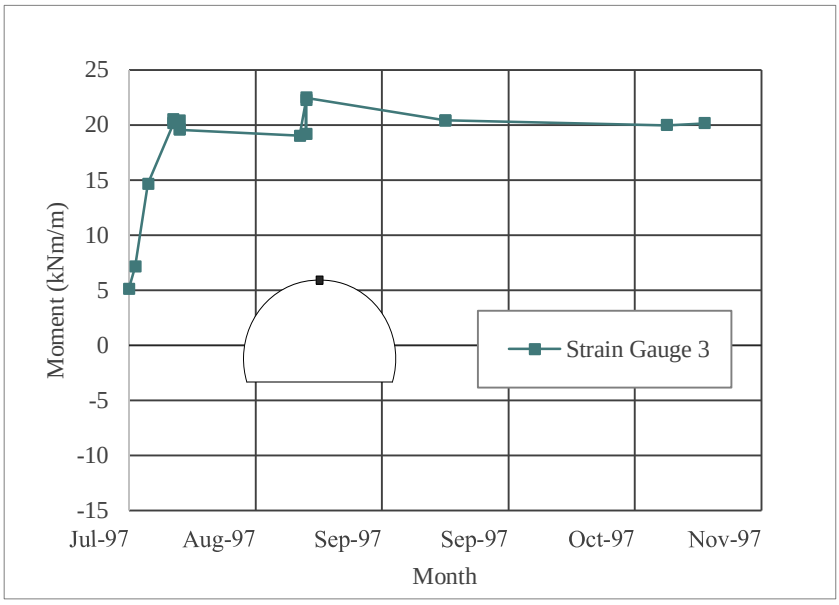

Figure 5.19. Moment measured in strain gauge 3 in the Furulund bru structure.

The measured moment in the side- wall is presented in Figure 5.20. The measurements are relatively consistent. At completion the moment in strain gauge 2 is -12.8 kNm/m, corresponding with the moment in strain gauge 4 is -12.2 kNm/m. During construction the lowest moment was measured in strain gauge 2 with a value of -14.3 kNm/m.

The measured moment in the footing is presented in Figure 5.21. The measurement has a constant break of roughly 3.5 kNm/m. At completed construction the moment in strain gauge 1 is 10.5 kNm/m and the corresponding measurement in strain gauge 5 is 7.0 kNm/m.

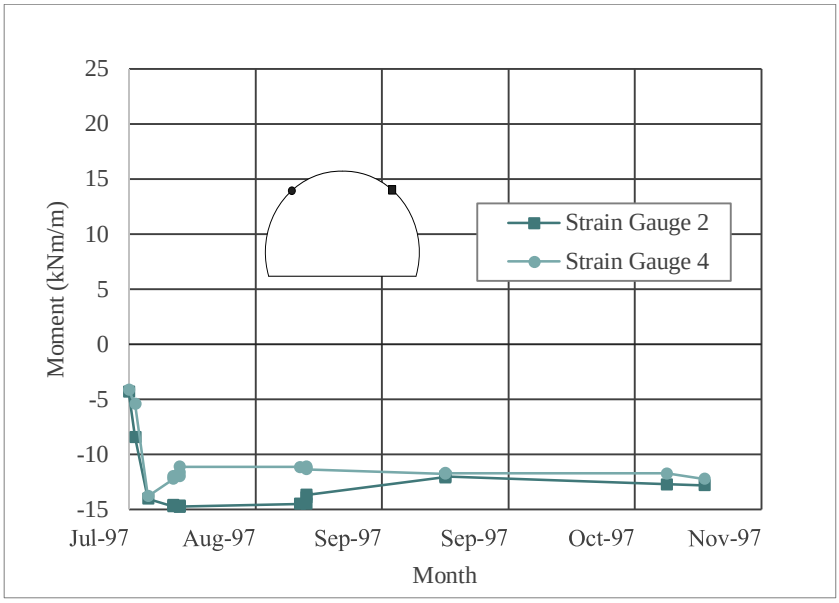

Figure 5.20 Moment measured in strain gauge 2 and 4 in the Furulund bru structure.

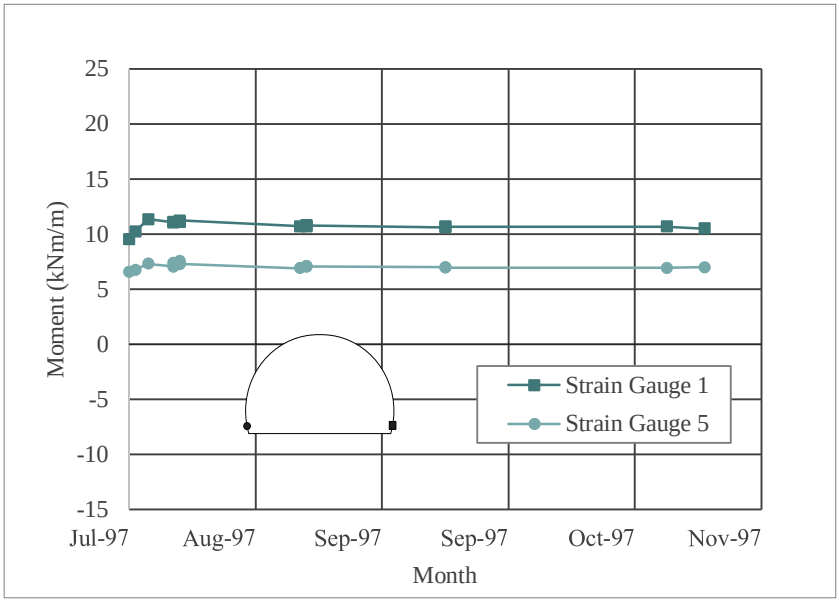

Figure 5.21 Moment measured in strain gauge 1 and 5 in the Furulund bru structure.

5.2.2. Modeling with PLAXIS 2D

The final geometry for Furulund bru before calculation is presented in Figure 5.22. Figure 5.23 shows the structure with 1.2 m cover, subsequently after calculation and deformation. The origin is placed in the centre of the structure in y-direction and in the footing of the steel structure in x-direction.

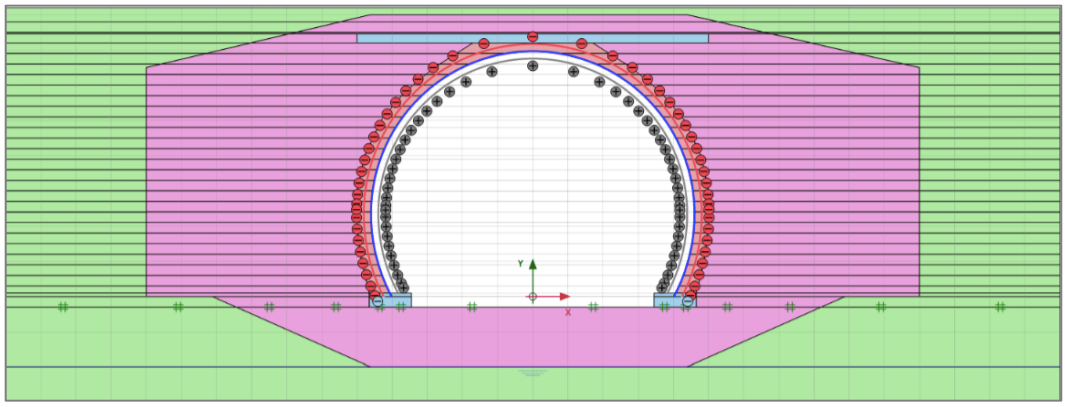

Figure 5.22. Final geometry of the Furulund bru structure modelled in PLAXIS 2D.

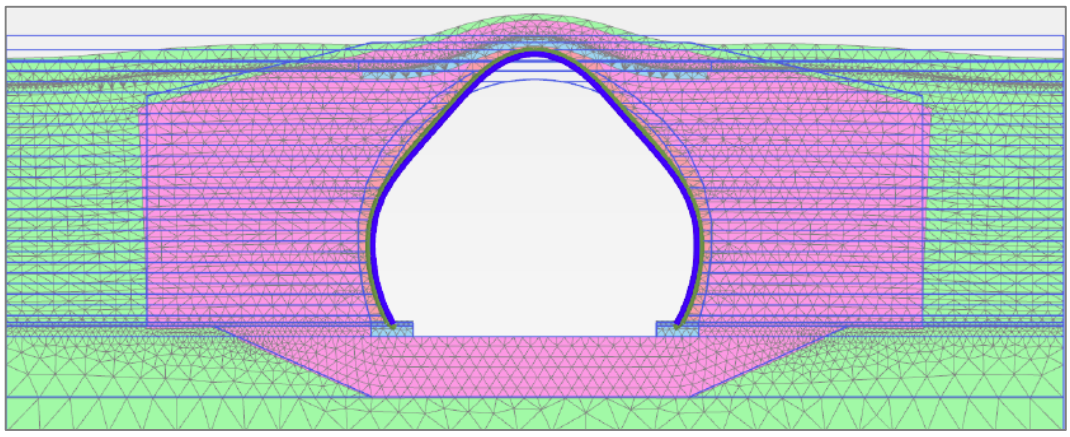

Figure 5.23. Furulund bru with 1.2 m cover after completed calculation. Deformation is scaled up 50 times.

The modelled earth pressure is presented in
Table 3. The vertical earth pressure in the backfilling is significantly higher than the horizontal earth pressure. In the crown the modelled value shows 5.1 kN/m^2 with a 0.5 m cover, and a value almost three times higher with a cover of 1.2 m. In cell 3 the earth pressure is modelled to 32.9 kN/m^2 with 0.5 cover, and an increase to 52.5 kN/m^2 with 1.2 m cover.

Table 3. Modelled earth pressure on the Furulund bru structure.

	Soil	X [m]	Y [m]	σ_{ep} [kN/m^2] Cover: 0.5 m	Cover: 1.2 m
Cell 2	Gravel 0-16	4.8	3.9	22.6	37.1
Cell 1	Gravel 0-16	4.8	3.9	98.8	116.0
Cell 4	Gravel 0-16	0.0	7.0	5.1	14.9
Cell 3	Gravel 0-17	2.9	6.0	32.9	52.5

The modelled axial force and moment in the positions of the strain gauges is presented in Table 4. A visualization of the forces is presented in Figure 5.24 and Figure 5.25. The axial force is greatest in the footing and decrease towards the crown. The maximum axial force with a 0.5 cover is 212.7 kN/m^{2,} and 271.6 kN/m^2 with 1.2 cover. The lowest value is 64.5 kN/m^2 and 104.3 kN/m^2. The moment is largest in the crown with a value of -5.5 kNm/m. In the footing the moment is modelled to a value of 0.4 kNm/m with 0.5 cover and 0.8 kNm/m with 1.2 cover.

Table 4 Modelled axial force and moment in the Furulund bru structure.

	X [m]	Y [m]	Axial force [kN/m] Cover: 0.5 m	Cover: 1.2 m	Moment [kNm/m] Cover: 0.5 m	Cover: 1.2 m
Strain gauge 3	0.0	7.0	64.5	104.3	-5.5	-5.4
Strain gauge 2	3.8	5.0	105.4	173.5	2.6	2.5
Strain gauge 4	-3.8	5.0	105.4	173.5	2.6	2.5
Strain gauge 1	4.1	0.2	212.6	271.6	0.4	0.8
Strain gauge 5	-4.1	0.2	212.7	271.7	0.4	0.8

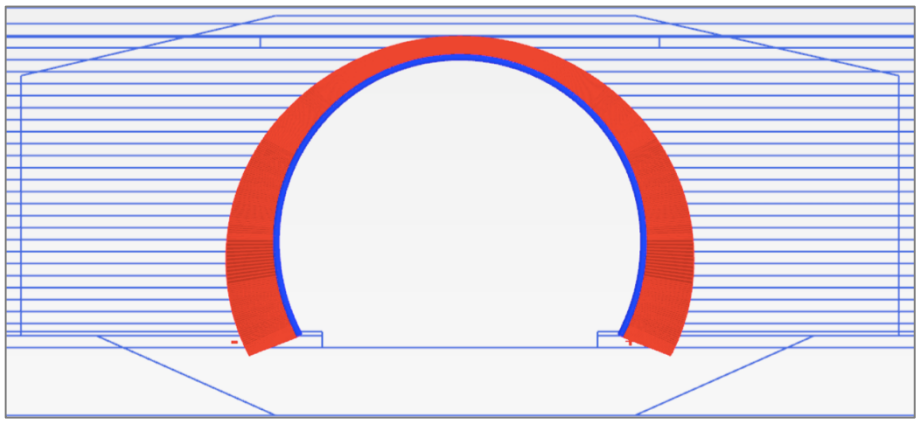

Figure 5.24 Modelled Axial force in the Furulund bru structure with 1.2 m cover.

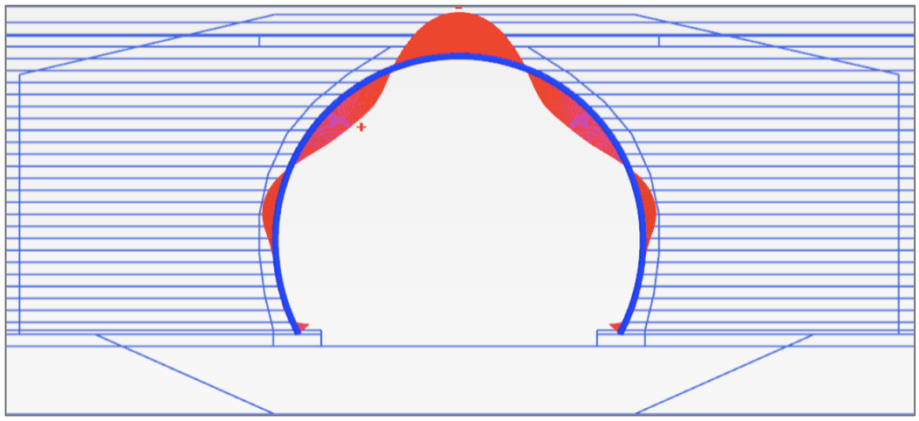

Figure 5.25 Modelled moment in the Furulund bru structure with 1.2 m cover.

The vertical deformation is visualized in Figure 5.26. The deflection is larger with 0.5 m cover than with 1.2 m cover, subsequently 15.3 mm and 14.2 mm.

The horizontal deflection is visualized in Figure 5.27. The horizontal deformation is larges 4.5 m over ground zero. The diversity between 0.5 cover and 1.2 cover is small, with values of subsequently -7.6 mm and -7.3 mm deformation.

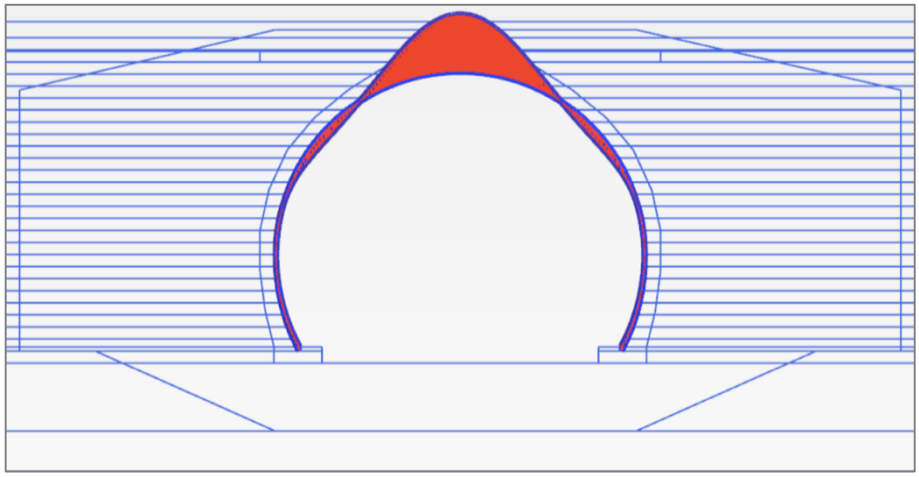

Figure 5.26. Modelled vertical deformation in the Furulund bru structure with 1.2 m cover. Scaled up 50 times.

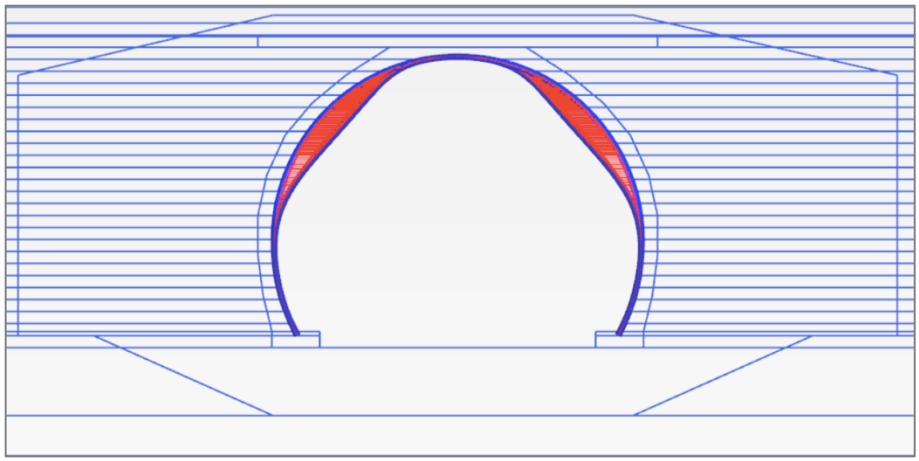

Figure 5.27 Modelled horizontal deformation in the structure Furulund bru with 1.2 m cover. Scaled up 50 times.

5.2.3. Final Results

A systematisation of results is presented in Table 5.

Table 5 Systematisation of result for the structure Furulund bru.

	Measured value after completed structure	Measured value, summer 2015	Modelled values in PLAXIS 2D Cover: 0.5 m	Cover: 1.2 m	Hand calculations	
Earth pressure Cell 2	11.0	13.0	22.6	37.1	-	kN/m^2
Earth pressure Cell 1	119.0	136.0	98.8	116	-	kN/m^2
Earth pressure cell 4	0.0	9.0	5.1	14.9	-	kN/m^2
Earth pressure Cell 3	25.0	48.0*	32.9	52.5	-	kN/m^2
Axial force Strain gauge 3	333.4	-	64.5	104.3	306.4**	kN/m
Axial force Strain gauge 2	36.6	-	105.4	173.5	-	kN/m
Axial force Strain gauge 4	178.4	-	105.4	173.5	-	kN/m
Axial force Strain gauge 1	60.9	-	212.6	271.6	-	kN/m
Axial force Strain gauge 5	60.9	-	212.7	271.7	-	kN/m
Moment Strain gauge 3	20.1	-	-5.5	-5.4	-15.4***	kNm/m
Moment Strain gauge 2	-12.8	-	2.6	2.5	-	kNm/m
Moment Strain gauge 4	-12.2	-	2.6	2.5	-	kNm/m
Moment Strain gauge 1	10.5	-	0.4	0.8	-	kNm/m
Moment Strain gauge 5	7.0	-	0.4	0.8	-	kNm/m
Crown, vertical deformation	-	-	15.3	14.2	14.5	mm
Horizontal deformation	-	-	-7.6	-7.3	9	mm

* Measurement from 1999 due to inconclusive measurement in 2015

** Maximum axial force

*** Maximum moment

6. Discussion

6.1. Earth Pressure

The measured earth pressure showed larger values in 2015 than the measurements taken after the structure was completed. The soil requires time to settle, and as a consequent the pressure distribution is altered. Over time the soil will stabilize and the earth pressure curve level out. The modeling should therefore reflect the long-term measurements to ensure the quality of the soil- steel structure throughout its lifetime. The basis for comparison is consequently reflecting the most resent measurements, in this case the measurements of 2015.

At the Dovre structure the earth pressure on the side-walls have a modelled value of 111% of the maximum value measured. The earth pressure in the crown and underneath the steel structure have larger errors, and subsequently the modelled value is 43% and 146% of the value measured. The model in PLAXIS 2D is not fitted to the exact placement of the earth pressure cells in respect to cover height. This could be a reason for the inaccuracy in cell 1, 3 and 6.

The largest error is found in the crown. This is the only modelled value at the Dovre structure which is lower than the corresponding measurement. Calculated overburden pressure is estimated to 70 kN/m^2, and hence the modelled value is 40% of the overburden pressure. The arching effect was described in chapter 2.1.2 and could explain why the modelled earth pressure decreased. If this is the case, the positive arching modelled is greater than the values measured. Chevalier, Combe and Villard (2007) described how the arching effect depends on the friction behaviour and the boundary conditions of the soil. The material model used for the modeling is Mohr Coulomb, and is based on limited parameters. To accomplish a more accurate material model, laboratory testing is required and could improve the modelled results.

At Furulund Bru the model was tested for a structure with minimum and recommended covers. Not surprisingly, the highest earth pressure was found in the modelled structure with a cover of 1.2 m. A rough estimation of the cover height shows 0.8 m. The correspondence between the measured and modelled values in cell 3 and 4 strengthens this assumption.

The measured values in the backfill have larger inaccuracy. Notice that the horizontally measured value is lower, and that the vertically measured value is higher than the modelled

value. The explanation is therefore not likely to be based on inaccurate placements of modelled values concerning ‘in situ’ cell locations. The geometry of the backfill and soil parameters in the model was based on theoretical assumptions and could therefore be a source of error. In a case where the modeling was performed before the construction, this would not be a problem because the structure ‘in situ’ would have been built as projected.

6.2. Axial Stress and Moment in the Steel Structure

The modelled axial stress at Furulund bru appears to be inverted in comparison to the values measured. Both the measured axial force and moment are higher than the modelled value. In PLAXIS 2D the steel structure is modelled with plain steel plates. The plates are given attributes to imitate the corrugation, but the actual geometry is absent. The force distribution on the steel structure is therefore not identical.

The measurements of axial force and moment are performed by measuring the strain in the top and base of the corrugation and is thereby specified for selected corrugations. The measurements could therefore be inconsistent with the overall force distribution. The axial force measured in strain gauge 2 and 4 at Furulund bru demonstrate how unreliable these measurements can be. To develop an understanding of the internal force distribution in the steel structure additional corrugations have to be measured and compared in respect to the entire structure. It is possible that the modelled structure better reflects the total distribution of forces. Extra measurements will however be required in order to test such a hypothesis.

The estimation method based on Pettersson and Sundquist (2007) gives an adequate approximation on the maximum axial force and moment. It is however peculiar that the hand calculations present a better representation of the measurements at Furulund bru than the model in PLAXIS 2D, considering that the reliving slab is excluded. The hand calculations do however have a disadvantage, as the distribution of axial force and moment are not included.

6.3. Deformations in the Steel Structure

The measurements on deformation at the Dovre structure vary over time. In 1987 the deformation was 8 mm, then increased to 16 mm ten years later. From 2005 the measurements were stable and the deformation measured 8 mm in 2015. The deformation is dependent on temperature but it appears to be small correspondence relating to season. It would have been interesting to compare the results to mean annual temperature in order to

check for significant coherence. The modelled value in PLAXIS 2D show positive deformation, indicating span increase. The cause of the different outcome is probably a parameter error due to stiffness. To avoid this problem, the material properties must be modified. Another way to perhaps strengthen the simulation is to insert a line-load to each backfill layer to imitate the compression performed during backfill.

The measurements on horizontal deformation at the Dovre structure had a peak value of 35 mm during construction and decreased to 21 mm after completion. Machelski, Michalski and Janusz (2009) described how peaking is common and favourable during construction. Peaking in the steel structure creates a buffer to counteract posterior loads from cover and live-loads. All tough peaking is favoured; it is important to control that the tension in the steel caused by deformation is within the yield point. If the yield point is surpassed the deformation could cause permanent weakness in the structure. By modifying the material parameters, the model could give similar results. The detailed monitoring presented in PLAXIS 2D will be useful in future soil- steel bridges as the dimension increase and the features become more complex. It will then be essential with precise projecting in order to avoid complications during construction.

The equation set proposed by Machelski, Michalski and Janusz (2009) present an estimate of maximum deflection in the crown and horizontal deformation. The algorithms presented in this thesis are based solely on the above mentioned article. To fully understand their work additional sources and first hand information from the authors themselves are required. Despite the absence of complete understanding of their work, their algorithms produced a satisfactory approximation compared to the measured result at the Dovre structure.

7. Conclusions

The main goal of this thesis was to investigate the reliability of FEM modeling compared to short-term and long-term measurements. To perform the study two existing buried structures was examined; a closed form and an arch. Modeling was performed in PLAXIS 2D based on theoretical material properties and structure geometry.

The model gives an overall acceptable estimate of the earth pressure in a long-term perspective. The arching effect was higher in the model than ‘in situ’, suggesting that the material parameters in the backfill should be re-evaluated. To improve the model laboratory test on backfill soil is required. The internal forces in the steel structure did not correspond with the measurements. The measurements are performed on selected corrugations and might not display the total distribution of the internal forces. It would be interesting to do more measurements on tension in the steel structure to attain a better understanding of the internal force distribution. The measured deformation indicates a decrease in span while the modelled deformation shows an increase. To upgrade the model and perhaps get a better representation of deformation, inserting a line-load to each backfill layer is recommended.

Overall, the model in PLAXIS 2D produced adequate estimations of the earth pressure and internal forces. The detailed monitoring of the construction presented in the model could prove useful in future soil-steel structures. To obtain a representative model of the selected structures some additional adjustments are required.

8. Bibliography

Abdel-Sayed, G., Bakht, B. & Jaeger, L. G. (1993). *Soil-steel bridges: design and construction*. United States of America: McGraw-Hill, Inc. 357 pp.

Beben, D. (2009). Numerical analysis of a soil-steel bridge structure. *Baltic J Road & Bridge Eng*, 4 (1): 13-21.

Braaten, A., Oset, F. & Bruun, H. (2000). Furuland bru: fullskala belastningsforsøk på stålhvelv.

Chevalier, B., Combe, G. & Villard, P. (2007). Load transfers and arching effects in granular soil layer. *18ème Congrès Français de Mécanique (Grenoble 2007)*.

Duncan, J. M. (1978). Soil-culvert interaction method for design of metal culverts. *Transportation Research Record* (678).

Kunecki, B. & Kubica, E. (2004). Full-scale laboratory tests and FEM analysis of corrugated steel culverts under standardized railway load. *Archives of Civil and Mechanical Engineering*, 4 (4): 41-53.

Kunecki, B., Vaslestad, J. & Emdal, A. (2006). Long-term earth pressure measurements of two largespan flexible culverts in Norway.

Lefebvre, G., Laliberté, M., Lefebvre, L. M., Lafleur, J. & Fisher, C. (1976). Measurement of soil arching above a large diameter flexible culvert. *Canadian Geotechnical Journal*, 13 (1): 58-71.

Machelski, C., Michalski, J. & Janusz, L. (2009). Deformation factors of buried corrugated structures. *Transportation Research Record: Journal of the Transportation Research Board* (2116): 70-75.

Norsk Stål AS. (2016). Tabller og Standarder.

Peck, O. K. & Peck, R. B. (1948). *Earth pressure against underground constructions. Experience with flexible culverts through railroad embankments*. Proc. 2nd International conference on soil mechanics and foundation engineering, Rotterdam. 95-98 pp.

Pettersson, L. & Sundquist, H. (2007). Design of soil steel composite bridges. *Dept. for Architectural and civil engineering,, Royal Institute of Technology, KTH, Stockholm, Sweden*.

PLAXIS 2D. (2015). Tutorial Manual

Selig, E. T., Lockhart, C. W. & Lautensleger, R. W. (1980). Measured performance of newtown creek culvert. *Journal of Geotechnical and Geoenvironmental Engineering*, 106 (ASCE 15829).

Shimoseki, M., Kuwabara, T., Hamano, T. & Imaizumi, T. (2003). *FEM for Springs*: Springer Science & Business Media.

Szajna, W. S. (2007). Numerical model for the analysis of construction process of soil-steel culverts. *Archiwum Instytutu Inżynierii Lądowej/Politechnika Poznańska*: 215-223.

Taleb, B. & Moore, I. (1999). Metal culvert response to earth loading: Performance of two-dimensional analysis. *Transportation Research Record: Journal of the Transportation Research Board* (1656): 25-36.

Vaslestad, J. (1985). *Personal photograph. Dovre*.

Vaslestad, J. (1987). Super-spenn rør Dovre: observasjoner av jordtrykk, stålspenninger, deformasjoner og temperatur.

Vaslestad, J. (1989). Long-term behavior of flexible large-span culverts. *Transportation Research Record* (1231).

Vaslestad, J. (1990). Soil structure interaction of buried culverts. *Institutt for Geoteknikk, Norges Tekniske Hogskole, Universitetet I Trondheim*.

Vaslestad, J. (1997). Personal photograph. Sjoa.

Vegdirektoratet. (2014). HåndbokV220 - Geoteknikk i vegbygging, Statens vegvesen.

Vegdirektoratet. (2015). Håndbok N400 - Bruprosjektering , Statens vegvesen.

Wadi, H. (2012). *Soil Steel Composite Bridges: A comparison between the Pettersson-Sundquist design method and the Klöppel & Glock design method including finite element modeling*, Royal Institute of Technology (KTH), Department of Civil and Architectural Engineering, Division of Structural Engineering and Bridges, Stockholm, Sweden, .

Williams, K., MacKinnon, S. & Newhook, J. (2012). New and innovative developments for design and installation of deep corrugated buried flexible steel structures. *Archiwum Instytutu Inżynierii Lądowej/Politechnika Poznańska*: 265-274.

Yesuf, G. Y. (2016). *Personal Communication, Statens vegvesen, Oslo*

9. Appendix

9.1. Appendix 1

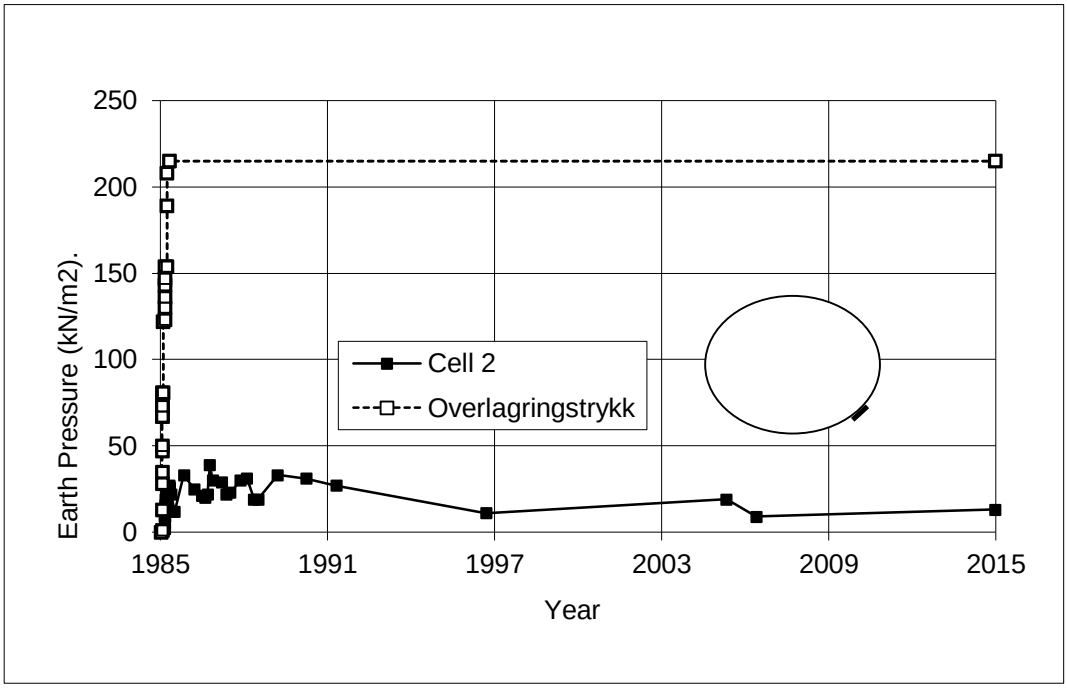

Figure 9.1 Measurements of earth pressure in cell 2 on the Dovre structure.

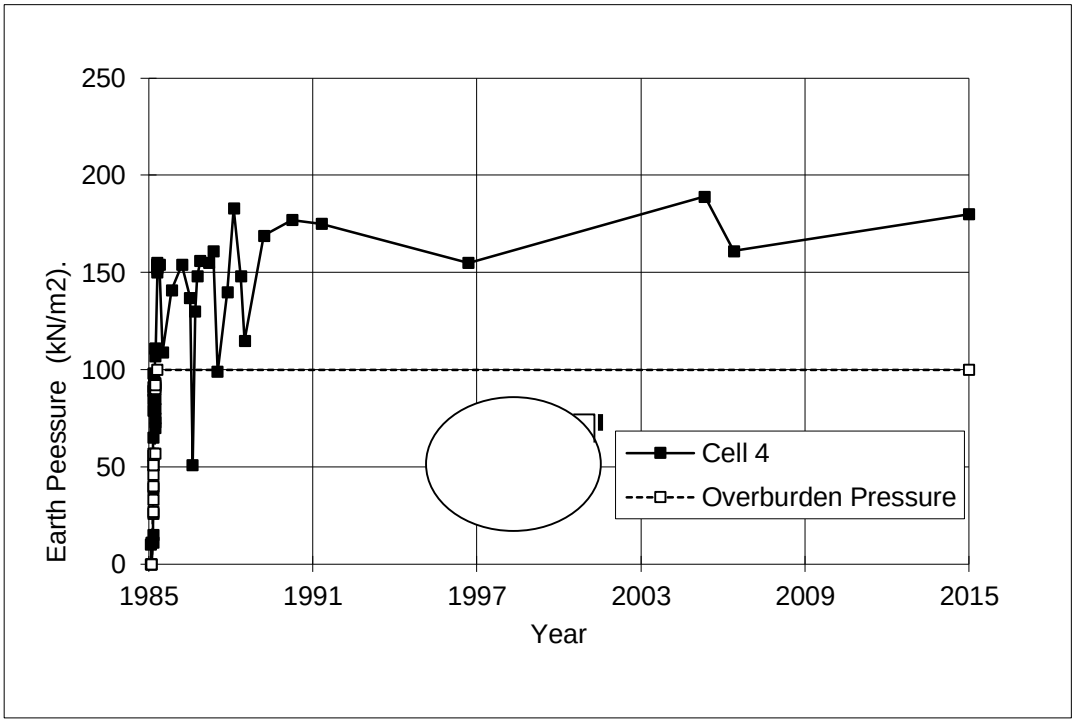

Figure 9.2 Measurements of earth pressure in cell 4 on the Dovre structure.

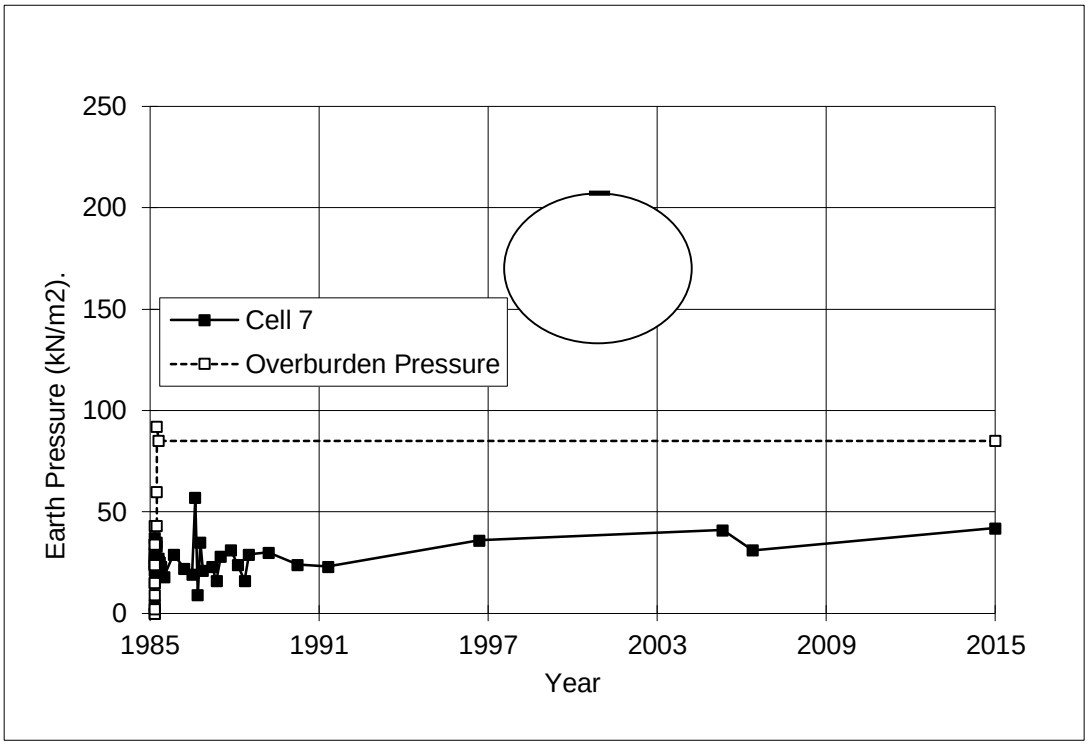

Figure 9.3 Measurements of earth pressure in cell 7 on the Dovre structure.

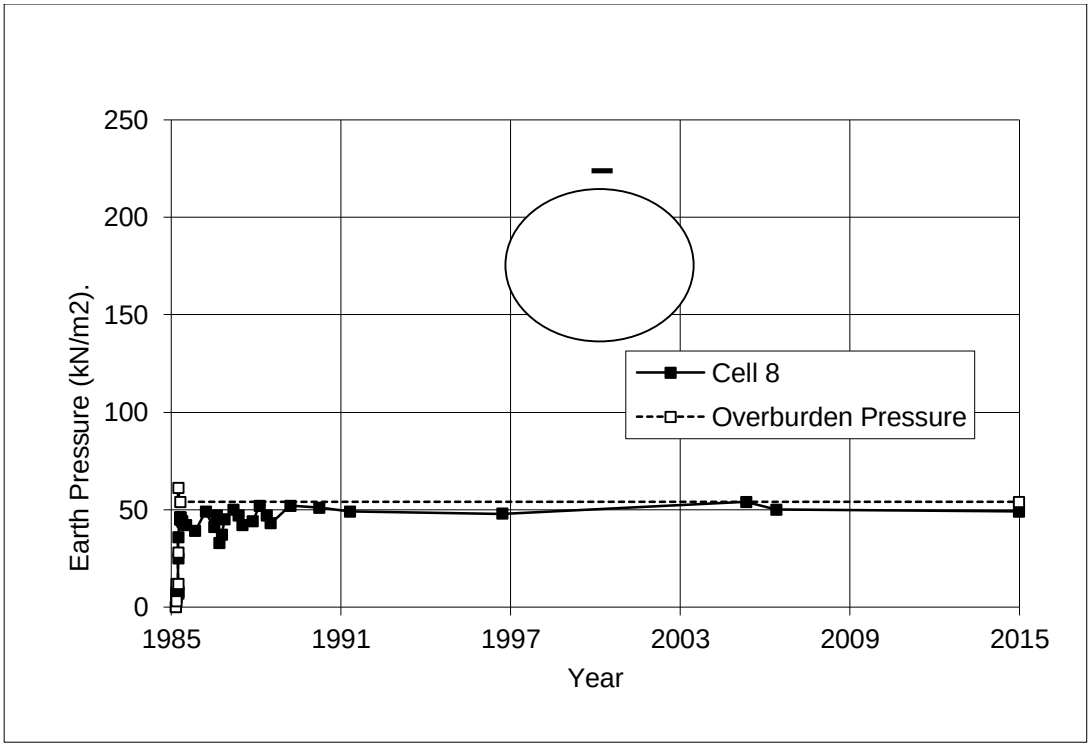

Figure 9.4 Measurements of earth pressure in cell 8 on the Dovre structure.

9.2. Appendix 2

Table 6 Material properties used in the PLAXIS 2D model

Parameter	Silt	Sand	Unit	
Material model	Mohr Coulomb	Mohr Coulomb	–	(Yesuf 2016)
Type of material behaviour	Drained	Drained	–	(Yesuf 2016)
Soil unit weight above phreatic level	18	17	kN/m3	(Vegdirektoratet 2015)
Soil unit weight below phreatic level	20	20	kN/m3	(PLAXIS 2D 2015)
Initial void ratio			–	
Young`s modulus	2,00E+04	1,30E+04	kN/m2	(PLAXIS 2D 2015)
Poisson`s ratio	0,3	0,3	–	(Yesuf 2016)
Cohesion	1	1	kN/m2	(PLAXIS 2D 2015)
Angle of internal friction	31	33	◦	(Vegdirektoratet 2015)
Dilatancy angle	0	0	◦	(Yesuf 2016)

Parameter	Gravel 0-16	Gravel 0-100	Unit	
Material model	Mohr Coulomb	Mohr Coulomb	–	(Yesuf 2016)
Type of material behaviour	Drained	Drained	–	(Yesuf 2016)
Soil unit weight above phreatic level	21,3858	20,7972	kN/m3	(Vaslestad 1987)
Soil unit weight below phreatic level	23,00445	22,4649	kN/m3	(Vaslestad 1987)
Initial void ratio			–	
Young`s modulus	8,04E+04	1,76E+05	kN/m2	Calculated from Eq.4.1
Poisson`s ratio	0,3	0,3	–	(Yesuf 2016)
Cohesion	31	54	kN/m2	(Vaslestad 1987)
Angle of internal friction	40	38	◦	(Vegdirektoratet 2015)
Dilatancy angle	0	0	◦	(Yesuf 2016)

Parameter	Moraine	Concrete	Unit	
Material model	Mohr Coulomb	Linear elastic	–	(Yesuf 2016)
Type of material behaviour	Drained	Non-porous	–	(Yesuf 2016)
Soil unit weight above phreatic level	19*	25	kN/m3	(Vegdirektoratet 2015)
Soil unit weight below phreatic level	21*	25	kN/m3	(Vegdirektoratet 2015)
Initial void ratio			–	
Young`s modulus	3,00E+04*	3,50E+07	kN/m2	(Vegdirektoratet 2015)
Poisson`s ratio	0,3	0,15	–	(Yesuf 2016)
Cohesion	1*		kN/m2	
Angle of internal friction	32*		◦	
Dilatancy angle	0		◦	(Yesuf 2016)

* Assumed parameters from parameters found in Vegdirektoratet (2014)

Table 7 Material properties for steel used in the PLAXIS 2D model

Parameter	Steel		
Material model	Elastoplastic		
Isotropic	yes		(Yesuf 2016)
End bearing	No		
EA1	1,74E+06	kN/m	(Vaslestad 1987; Vegdirektoratet 2014)
EA2	1,74E+06	kN/m	(Vaslestad 1987; Vegdirektoratet 2014)
EI	674	kNm2/m	(Vegdirektoratet 2014)
d	0,007	m	(Vaslestad 1987)
w	0,00638	kN/m/m	w=A*p*g
v (Poissons ratio)	0,3		
A	0,0082	m2/m	(Vegdirektoratet 2014)
p (unit weight)	7,85	kg/m3	(Norsk Stål AS 2016)
g (gravity)	9,81	m/s2	

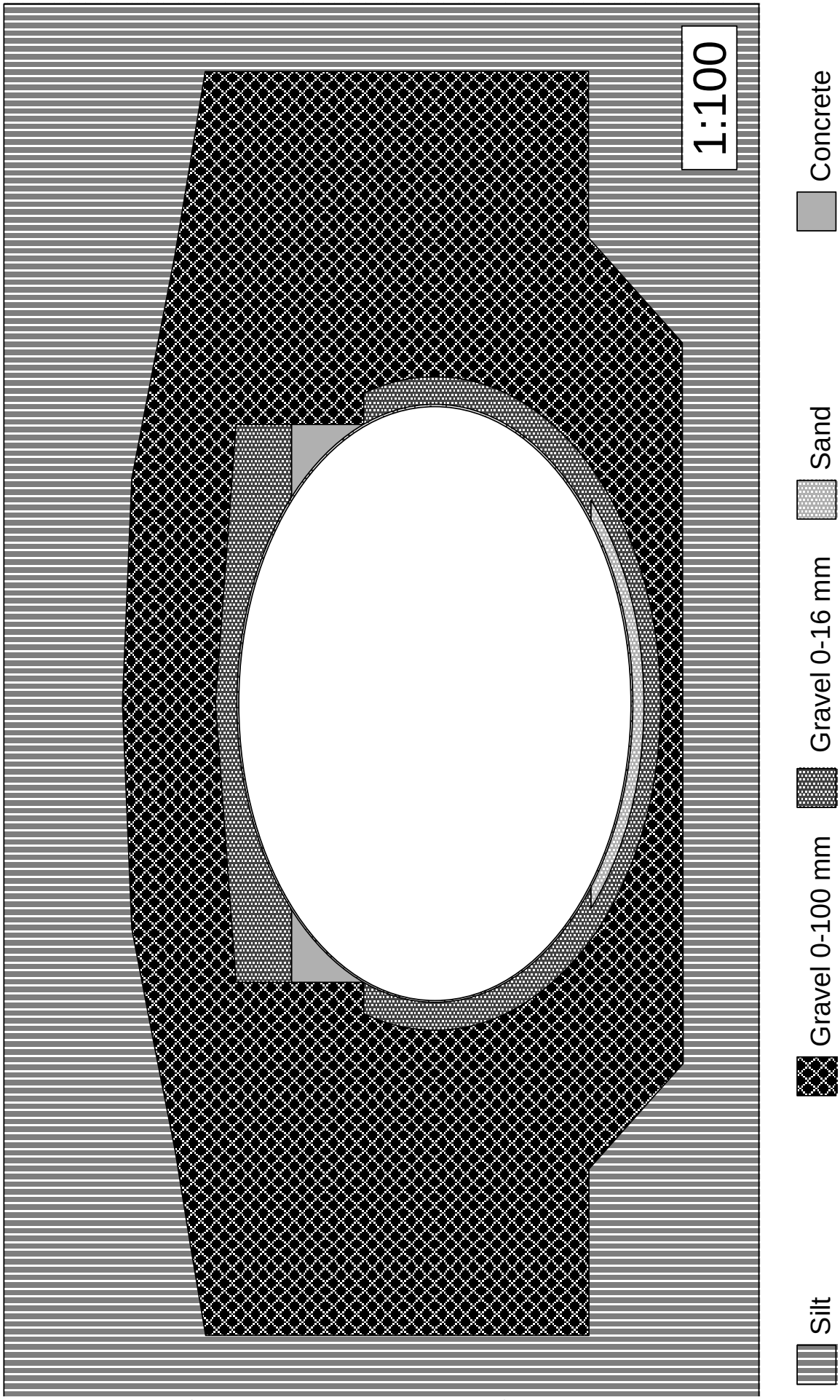

Figure 9.5 Cross section of the Dovre structure including description of the soil geometry 1:100.

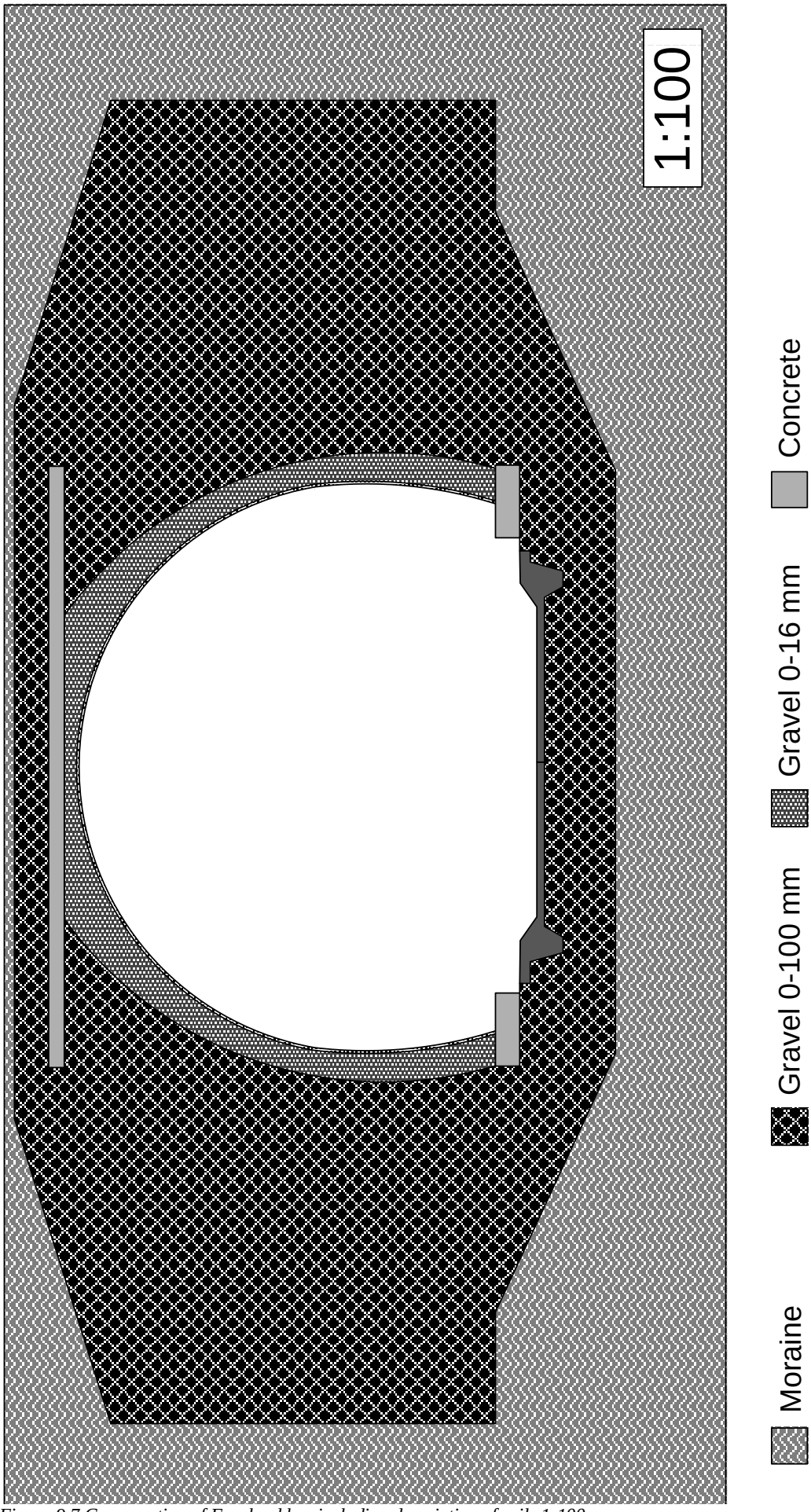

Figure 9.7 Cross section of Furulund bru including description of soils 1:100.

9.3. Appendix 3

Table 8 Parameters, assumptions and calculated results from the methods based on Pettersson and Sundquist (2007) and Machelski et. al (2009).

Parameter	The Dovre Structure	The Furulund bru Structure	Unit	Comment
γ_n	1	1		
E_s	2,10E+08	2,10E+08	kN/m^2	Kilde(Vegdirektoratet 2014)
a	0,2	0,2	m	
I_s	3,208E-06	3,208E-06	m^4/m	Kilde(Vegdirektoratet 2014)
γ_m	1,3	1,3		
h_{rel}	7,13	7	m	
h_c	4,2	1,2		
γ_b	21	21	kN/m^3	Kilde(Vaslestad 1987)
γ_c	21	21	kN/m^3	Kilde(Vaslestad 1987)
D	10,73	9,5	m	
h_D	3,565	4,6	m	
$h_{c,red}$	4,2	1,2	m	
$\varphi_{cover,d}$	39	39	°	Kilde(Vegdirektoratet 2014)
$\varphi_{cover,r}$	0,8603	0,8603	radian	Alteration from degrees
RP	99	99	%	Standard proctor for Gravel 0-100, kilde
E_b	1,76E+05	1,76E+05	kN/m^2	Calculated from Eq. 4.1
λ	6,455E+04	4,48E+04	/m	Calculated from Eq. 2.1
λ	2,48E+05	1,72E+05		Calculated from Eq.2.12
κ	0,66	0,74		Calculated from Eq. 2.2
K_w	2,5	3		Found from Figure 2.13
α	0,0007	0,0023		Calculated from Eq. 2.3 and 2.4
β	0,0004	0,0014		Found from the corrolation with β in Figure 2.14
Q	17,64	5,04	kN/m	Q = γ_b*h_c*a
w	0,0227	0,0145	m	Calculated from Eq. 2.3
u	0,0131	0,0090	m	Calculated from Eq. 2.5
S_{ar}	0,43	0,78		Found from Figure 2.15
f_1	0,7743	0,9173		Calculated subsequatnly from Eq. 2.8b and Eq. 2.8a
$f_{2,b}$	0,0009	0,0009		Found from Eq. 2.9b
$f_{2,c}$	0,0032	0,0032		Found from Eq. 2.10b
f_3	0,8758	1,8997		Calculated from Eq. 2.11
R_t	7,25	4,6	m	Found from manual testing
R_s	2,3	4,6	m	Found from manual testing
N_C	461,76	306,39	kN/m	Calculated from Eq. 2.6
M_C	6,52	-15,35	kNm/m	Calculated from Eq. 2.7

Norges miljø- og biovitenskapelig universitet
Noregs miljø- og biovitskapelege universitet
Norwegian University of Life Sciences

Postboks 5003
NO-1432 Ås
Norway